

1 **Supplementary Information for:**
2 **Super-resolution fight club: A broad assessment of 2D & 3D**
3 **single-molecule localization microscopy software**

4 *Daniel Sage*^{*+1}, *Thanh-An Pham*⁺¹, *Hazen Babcock*², *Tomas Lukes*³, *Thomas Pengo*⁴, *Ramraj Velmurugan*⁵, *Alex*
5 *Herbert*⁶, *Anurag Agrawal*⁷, *Silvia Colabrese*^{1,8}, *Ann Wheeler*⁹, *Anna Archetti*¹⁰, *Bernd Rieger*¹¹, *Raimund*
6 *Ober*⁵, *Guy M. Hagen*¹², *Jean-Baptiste Sibarita*¹³, *Jonas Ries*¹⁴, *Ricardo Henriques*¹⁵, *Michael Unser*¹, *Seamus*
7 *Holden*^{*+16}

8 *Corresponding authors: daniel.sage@epfl.ch, seamus.holden@ncl.ac.uk.

9 +Equal contribution

10 1: Biomedical Imaging Group, School of Engineering, Ecole Polytechnique Fédérale de Lausanne
11 (EPFL), Switzerland

12 2: Harvard Center for Advanced Imaging, Harvard University, Cambridge, Massachusetts, USA

13 3: Laboratory of Nanoscale Biology & Laboratoire d'Optique Biomédicale, STI - IBI, EPFL, Lausanne,
14 Switzerland

15 4: University of Minnesota Informatics Institute, University of Minnesota Twin Cities, USA

16 5: Electrical Engineering, University of Texas Dallas, Richardson, Texas, USA

17 6: MRC Genome Damage and Stability Centre, School of Life Sciences, University of Sussex, Brighton,
18 UK

19 7 : Double Helix LLC, Boulder, Colorado, USA

20 8 : Istituto Italiano di Tecnologia, Genova, Italy

21 9: Edinburgh Super-Resolution Imaging Consortium, University of Edinburgh, UK

22 10 : Laboratory of Experimental Biophysics, École Polytechnique Fédérale de Lausanne (EPFL),
23 Lausanne, Switzerland

24 11: Department of Imaging Physics, Faculty of Applied Sciences, Delft University of Technology, The
25 Netherlands

26 12: UCCS center for the Biofrontiers Institute, University of Colorado at Colorado Springs, Colorado,
27 USA

28 13: Institut Interdisciplinaire de Neurosciences, University of Bordeaux, France

29 14: European Molecular Biology Laboratory (EMBL), Cell Biology and Biophysics Unit, Heidelberg,
30 Germany

31 15: Quantitative Imaging and Nanobiophysics Group, MRC Laboratory for Molecular Cell Biology,
32 University College London, UK

33 16: Centre for Bacterial Cell Biology, Institute for Cell and Molecular Biosciences, Newcastle
34 University, UK

35

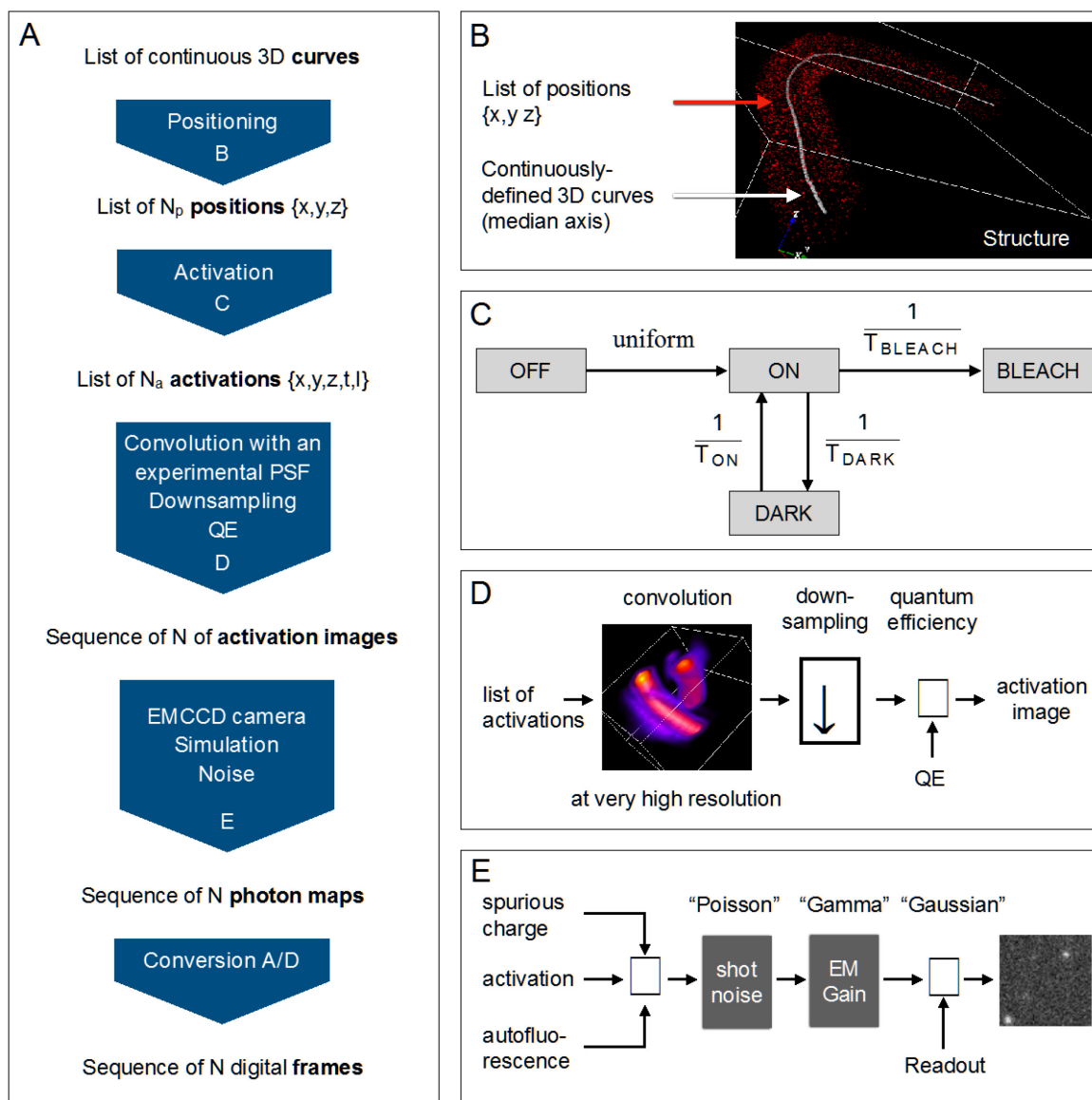
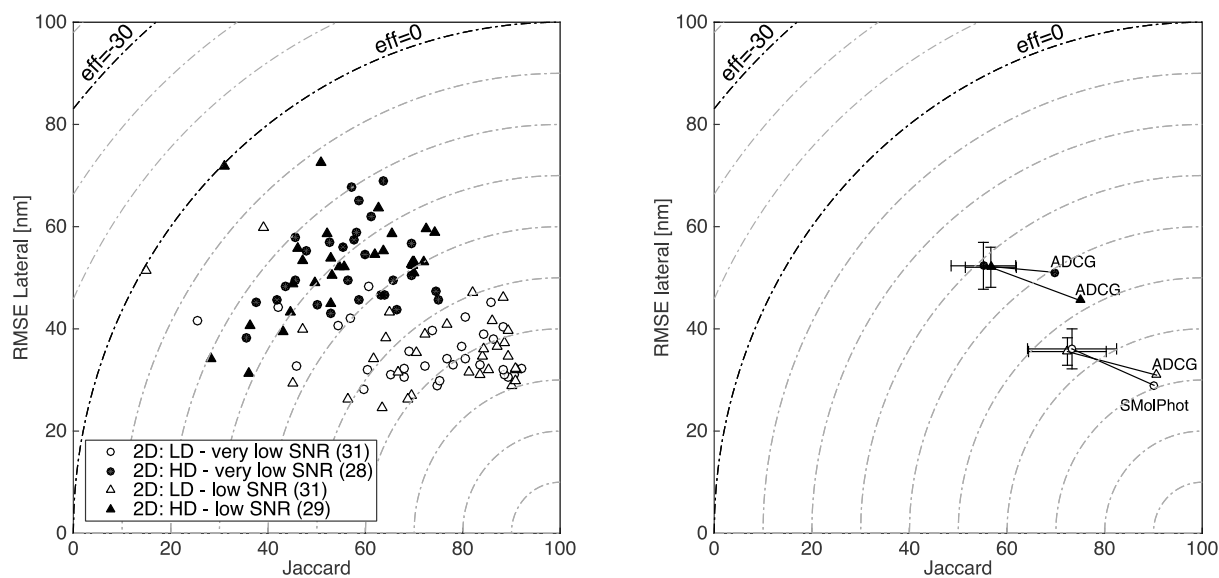


Figure S1: Simulations. **A.** The overall steps of the simulation are shown, from the 3D geometry of the structure to the sequence of digital frames. **B.** The geometry of the structure is constructed from a series of 3D tubes where every median axis of tubes (white line) is a 3D curve continuously defined by a three B-spline functions in the volume of interest. The membranes of the tubes are densely populated with possible positions of fluorophores according a given radius and a given thickness of membrane. **C.** The activation process takes the list of positions and activates the fluorophores following the 4-states model of activation. The parameters T_{BLEACH} , T_{ON} and T_{DARK} allow to control the blinking rate and the lifetime of the emitters. The output of the activation consist to a list of activations defined by a position (x,y,z) , a time (t) and a number of emitted photons (l) in the current frame. **D.** The creation of the sequence run frame-to-frame. All activations of a given frame are convolved with the experimental PSF at high resolution (2 nm), and reduced to the camera resolution. The number of photons per pixel is converted to electron by pixel using the quantum efficiency (QE) of the camera. **E.** The noise model is applied to the three sources of electrons: the activation of the emitters, the spurious charge of the camera and the autofluorescence background

53 (photons converted to electrons using QE). The shot noise follows a Poisson distribution; the EMCCD
54 gain is simulated by a Gamma function; and a Gaussian noise is added to simulate the read-out
55 noise. Finally, the acquired photons map at a given time are converted to digital frame in 16-bits, a
56 baseline is also added.



58
 59 **Figure S2: Comparison of 2D software performance.** Dashed lines indicate efficiency (higher is
 60 better). **A.** Performance of all 2D SMLM software. **B.** Average (marker with error bars) and best-in-
 61 class (marker with name) software performance for 2D modalities. LD, low density; HD, high density.

62

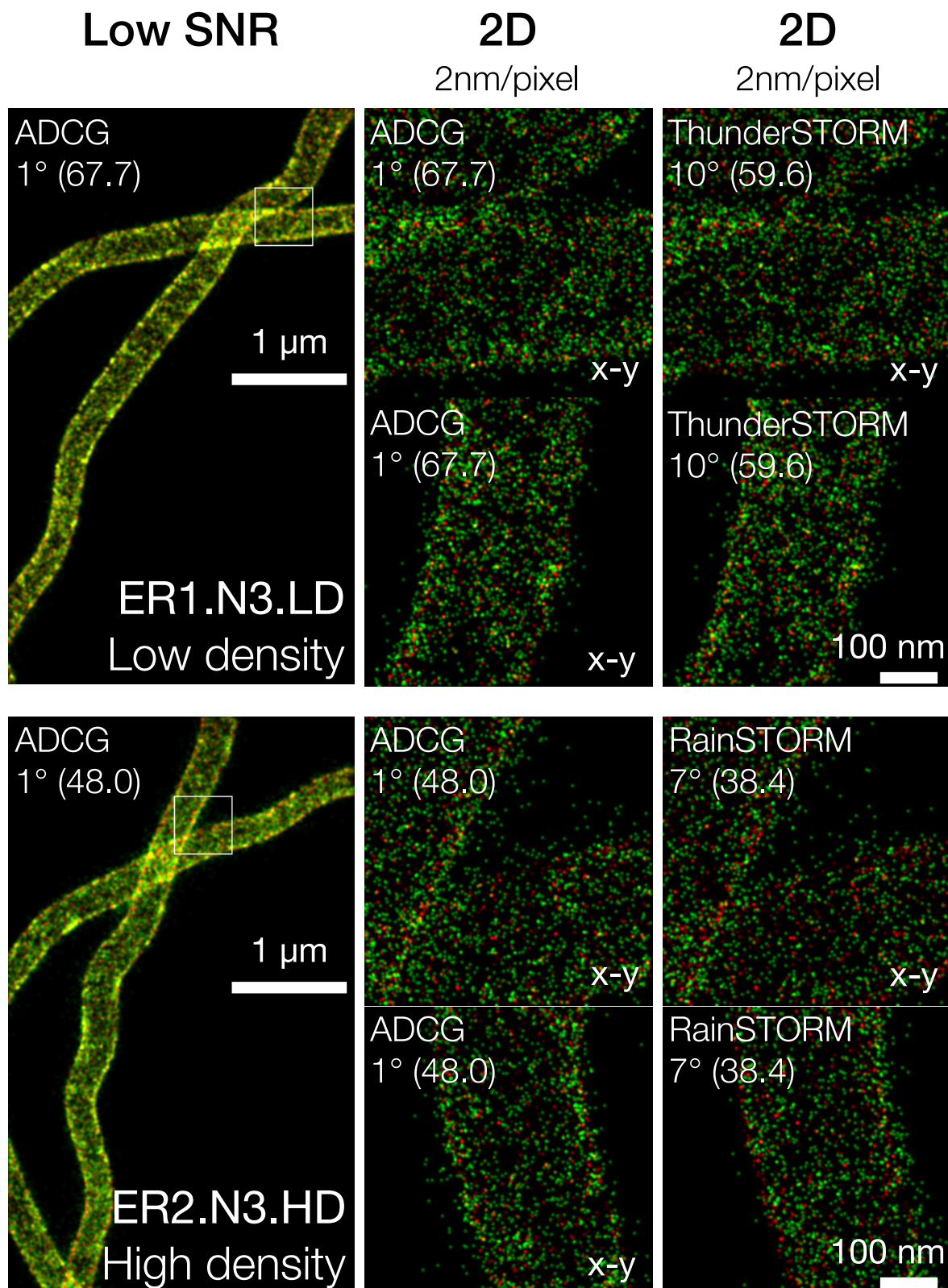
63

64

66

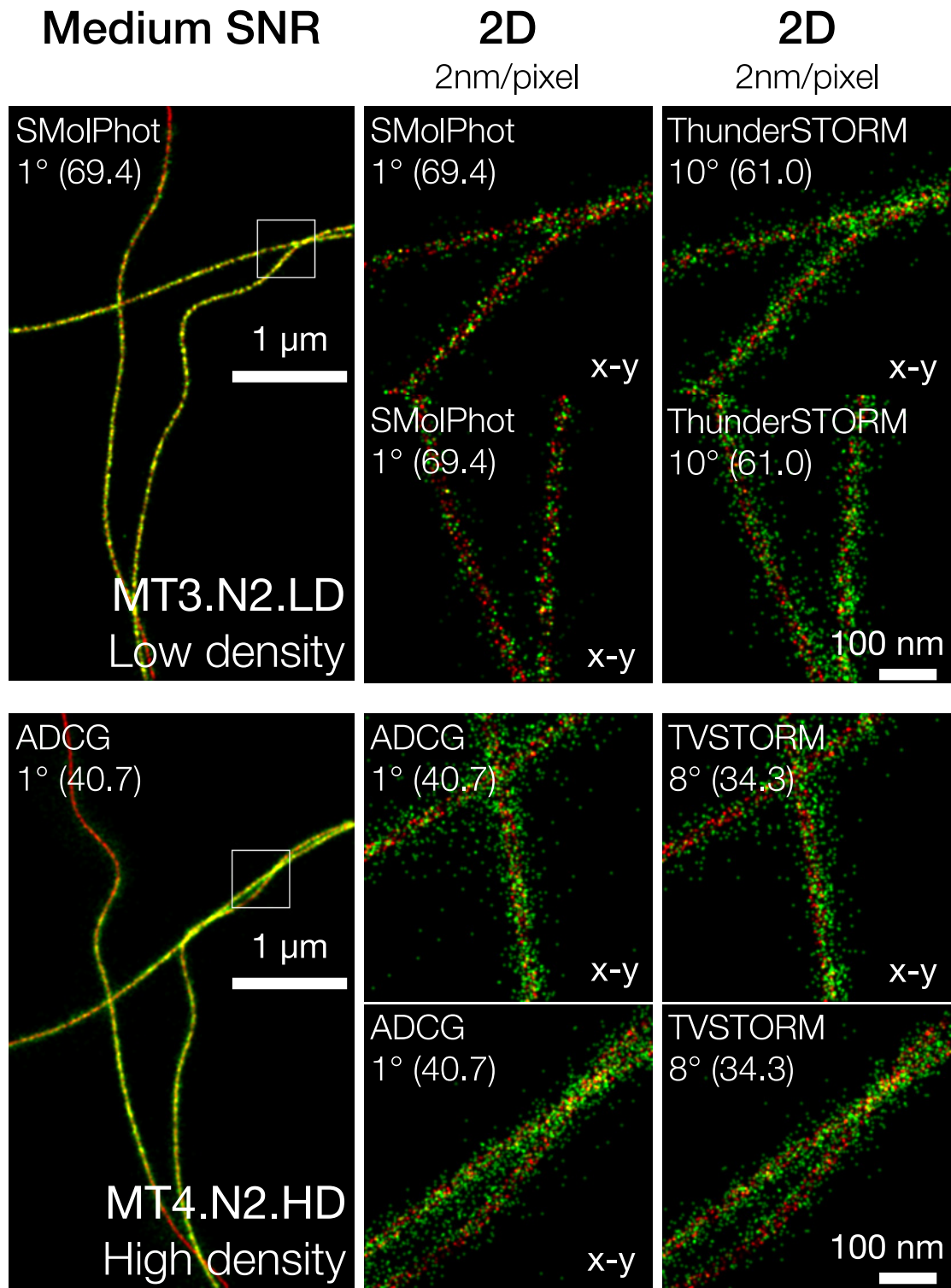
67 **Figure S3:** Super-resolved images of 3D competition datasets for best-in-class (top) and
68 representative average (bottom) software in each modality, for low SNR datasets. Box indicates
69 zoomed region. Red, ground truth; green, software results. Panel label key: *Software_name*
70 *Ranking*^o (*Efficiency*).

71



72

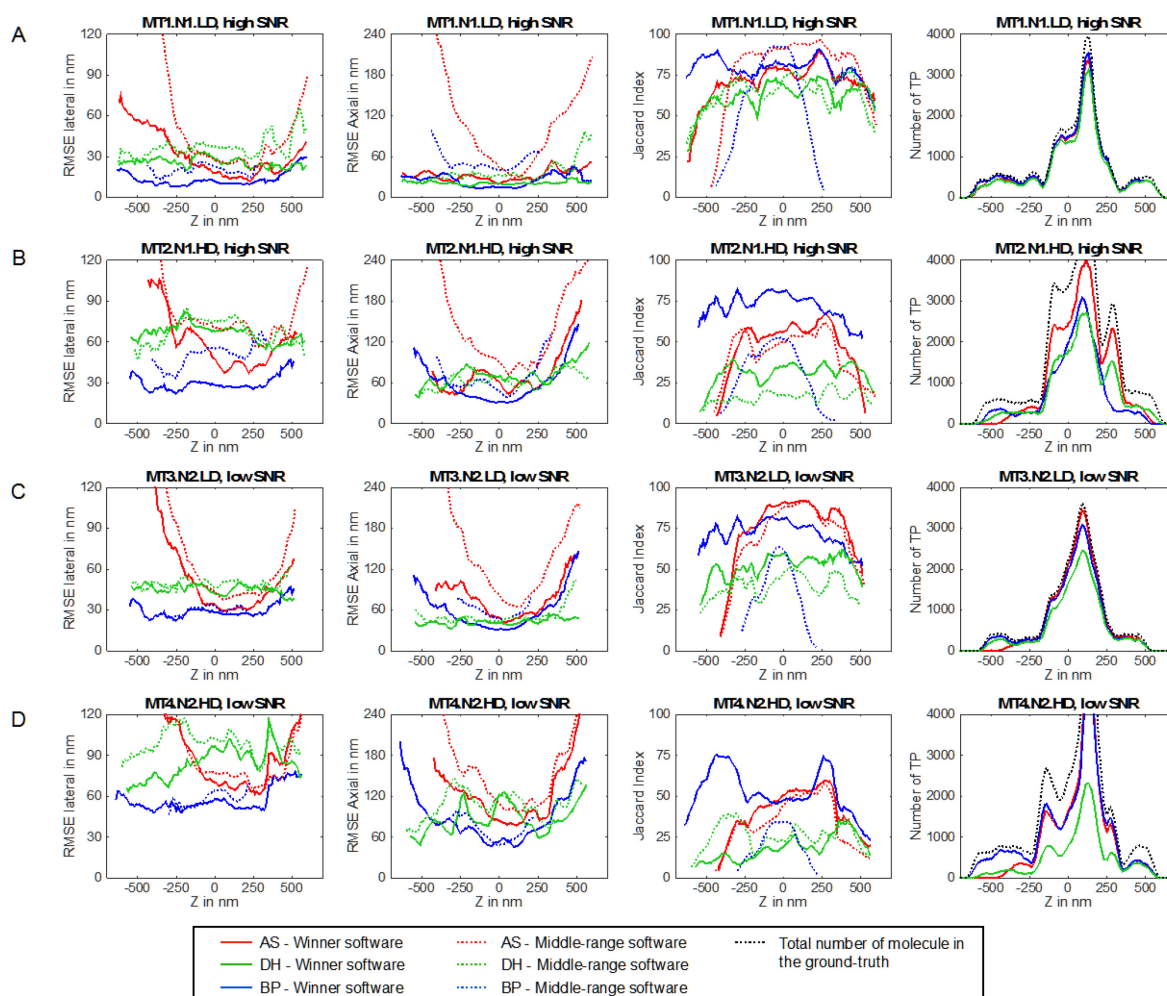
73 **Figure S4:** Super-resolved images of 2D competition datasets for best-in-class (top) and
 74 representative average (bottom) software in each modality, for low SNR pseudo-ER datasets. Box
 75 indicates zoomed region. Red, ground truth; green, software results. Panel label key:
 76 *Software_name Ranking° (Efficiency).*



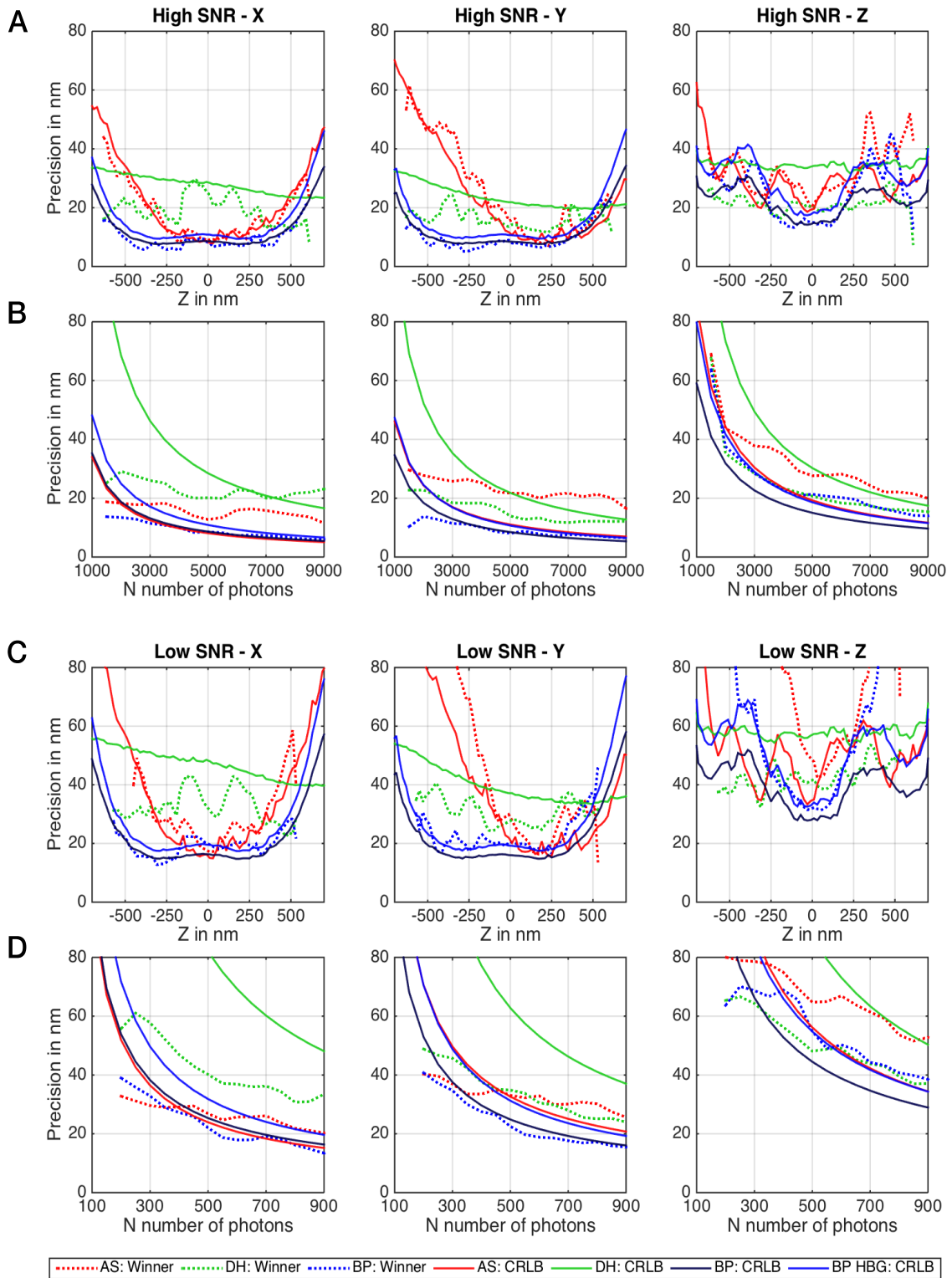
77
78
79
80
81

Figure S5: Super-resolved images of 2D competition datasets for best-in-class (top) and representative average (bottom) software in each modality, for medium SNR pseudo-microtubule datasets. Box indicates zoomed region. Red, ground truth; green, software results. Panel label key: *Software_name Ranking° (Efficiency)*.

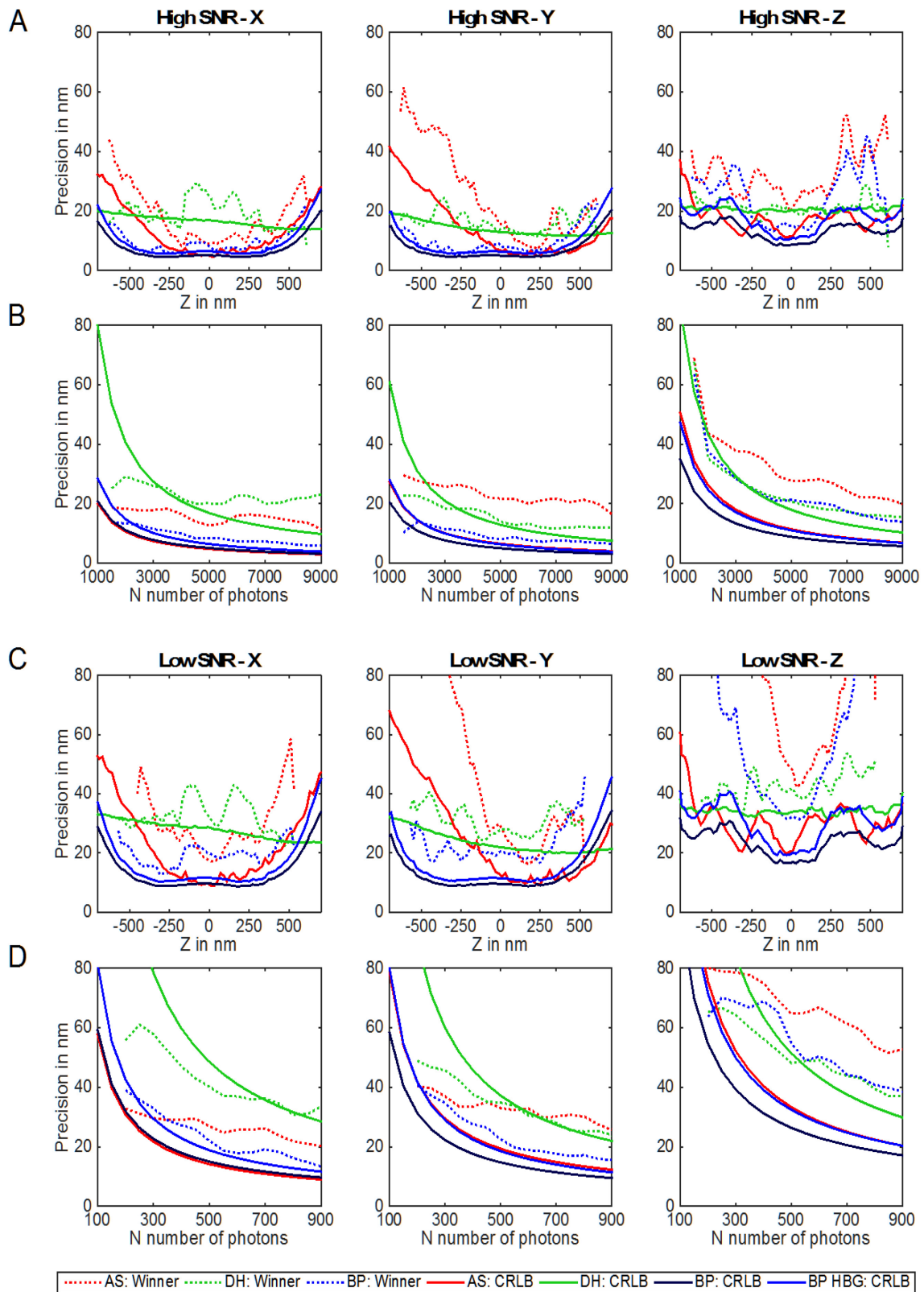
82



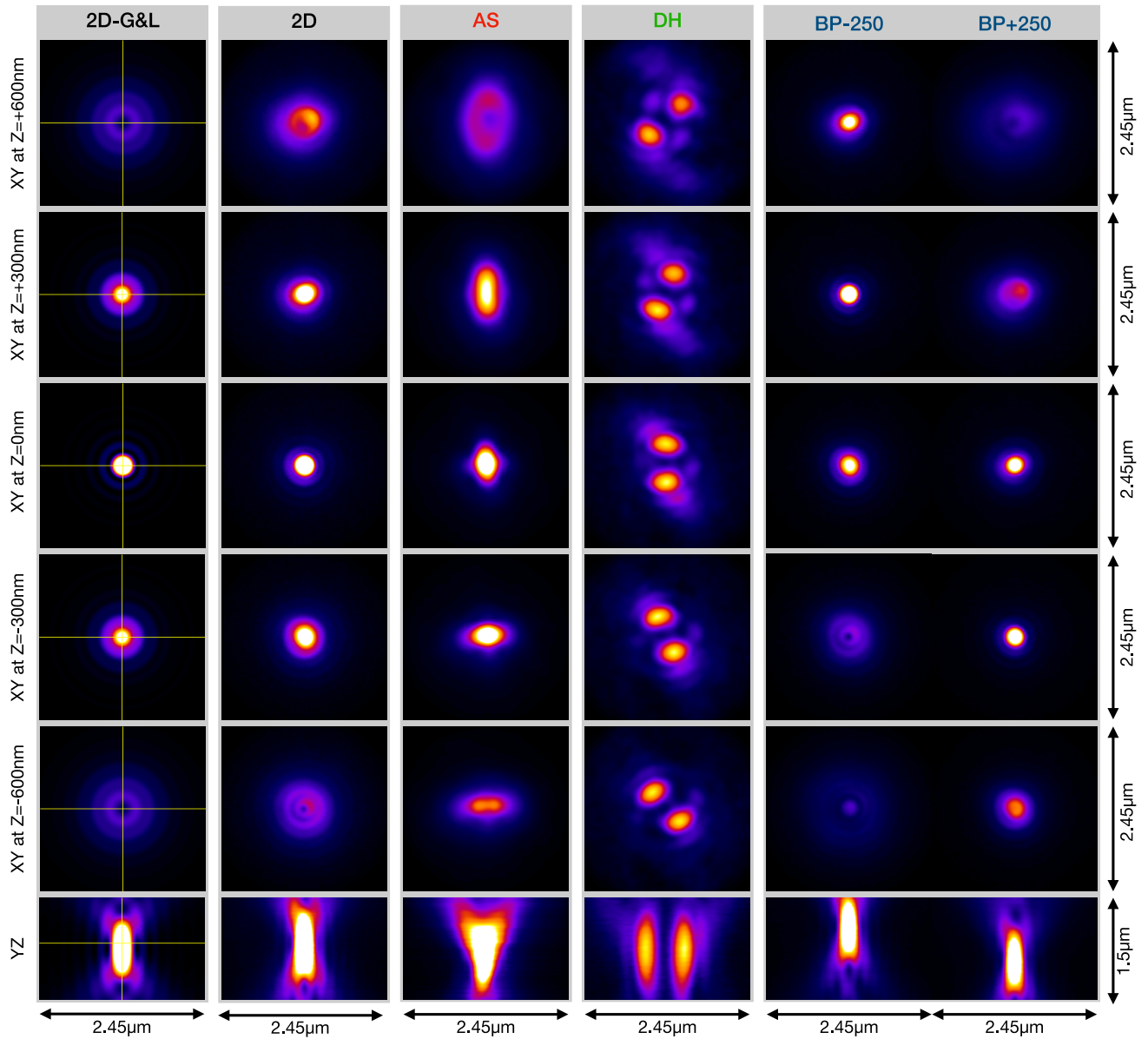
83
 84 **Figure S6:** 3D software performance as a function of depth Z (axial position of the molecule) for each
 85 competition dataset (A-D). The metrics are locally computed within a depth interval. Based on the
 86 true axial position of the molecules, we exclude the ones out of the depth interval of interest Z_i .
 87 From this subset and their (previously) paired software localisations, the lateral (1st column) and
 88 axial (2nd column) RMSE are computed. The Jaccard Index (3rd column) requires a false positive
 89 count for each bin, which is approximated using the non-paired software localisations that fall in Z_i .
 90 The winners (for AS, DH and BP in red, green and blue respectively (full line)) for each dataset
 91 MT1.N1.LD, MT2.N1.HD, MT3.N2.LD, MT4.N2.HD are plotted at the row 1 to 4 respectively. In
 92 addition, a software with average performance is also displayed for the metrics lateral and axial
 93 RMSE and the Jaccard Index (dotted line). The number of true positive (TP, 4th column) is the
 94 number of paired molecule included in Z_i . In addition to the winners, the total number of activations
 95 per depth interval is also displayed (Ground-truth, dotted black line).



99 **Figure S7:** Comparison inter-modality of the Cramer-Rao Lower Bounds (CRLB) in high SNR and low
100 SNR conditions on a single frame (without temporal grouping). For each condition, the RMSE
101 performance of the winning software is plotted for comparison with the CRLB limit^{1,2}. **A.** CRLB as a
102 function of the depth Z (axial position of the molecule) for noise condition N1 are computed with for
103 each PSF: astigmatism AS; double helix DH; biplane, BP, biplane high background BP HBG.
104 Calculations for AS, DH, BP were for a single molecule emitting $N=5'000$ photons on a frame with an
105 auto-fluorescence background $B=100$ photons for AS, DH and BP. The background used for the
106 biplane competition simulations had a higher background, $B=200$ (BP HBG, BP high background). **B.**
107 CRLBs as a function of the number of emitted photons N for noise condition N1 are computed for
108 each PSF (AS, DH, BP, BP HBG) for a single molecule at the focal plane ($Z=0$). **C.** CRLBs as a function of
109 depth Z for noise condition N2. **D.** CRLBs as a function of the number of emitted photons N for noise
110 condition N2. The CRLBs were computed based on the mathematical expression derived by Chao et
111 al.^{3,4}. The PSF are 10 nm spaced from which a cubic spline representation is computed over an area
112 of $6.4 \times 6.4 \mu\text{m}^2$. Contrarily to Chao et al. the PSFs were not regularized. As shown in Figure 1, our
113 acquisition model is similar to the one described by Chao et al. N is first convolved with the PSF and
114 integrated over each camera pixel. The background B is added to each pixel value (except the BP
115 modality for which we added $B/2$ to each pixel) and these quantities are then converted to an
116 electron count by multiplying them with the Quantum Efficiency ($QE = 0.9$). Some spurious charge
117 coming from the EMCCD camera (0.0002) is added to this quantity before applying a Poisson shot
118 noise n_{ie} . The noise from the EMCCD camera (gain $g = 300$) is modelled as a Gamma distribution with
119 the shape and scale parameters $k = n_{ie}$ and $\theta = g$ respectively. Finally, a zero mean Gaussian readout-
120 noise ($\sigma = 74.4$) is added. The analog-to-digital conversion is negligible and ignored for the
121 computation of the CRLB. Once the Fisher Information matrix is obtained⁴, the square root of the
122 diagonal of its inverse equals the CRLB. This setting corresponds to the MT1.N1.LD dataset.



124 **Figure S8:** Comparison of the winner with the Cramer-Rao Lower Bounds (CRLB), combining
125 localizations from multiple frames (temporal grouping), in high SNR and low SNR conditions. **A.** CRLB
126 as a function of the depth Z (axial position of the molecule) are computed for noise condition N1
127 with each PSF (AS, DH, BP in red, green, blue respectively) for a single molecule emitting $N=5'000$
128 photons per frame on $F = 2.85$ frames (average number of frames for which a molecule is activated)
129 with an auto-fluorescence background $B=100$ photons for AS, DH and BP. The BP was also displayed
130 for $B=200$ because it was the setting of the datasets of the competition (BP HBG). **B.** CRLB as a
131 function of the number of emitted photons N per frame for noise condition N1 are computed for
132 each PSF (AS, DH, BP, BP HBG) for a single molecule at the focal plane ($Z = 0$) for $F = 2.85$ frames
133 (average number of frames for which a molecule is activated). **C.** CRLBs as a function of depth Z for
134 noise condition N2 for $F = 2.85$ frames. **D.** CRLBs as a function of the number of emitted photons N
135 for noise condition N2 for $F = 2.85$ frames. The details of the computation of the CRLBs for a single
136 frame are in the legend of Fig. S7. The Fisher Information matrix (FIM) for a single frame is multiplied
137 by F and the square root of the diagonal of its inverse equals the CRLB.



139

140

141 **Figure S9:** XY and YZ profiles of experimentally derived competition PSFs for different imaging142 modalities compared with theoretical Gibson & Lanni PSF⁵. Experimentally derived PSFs were

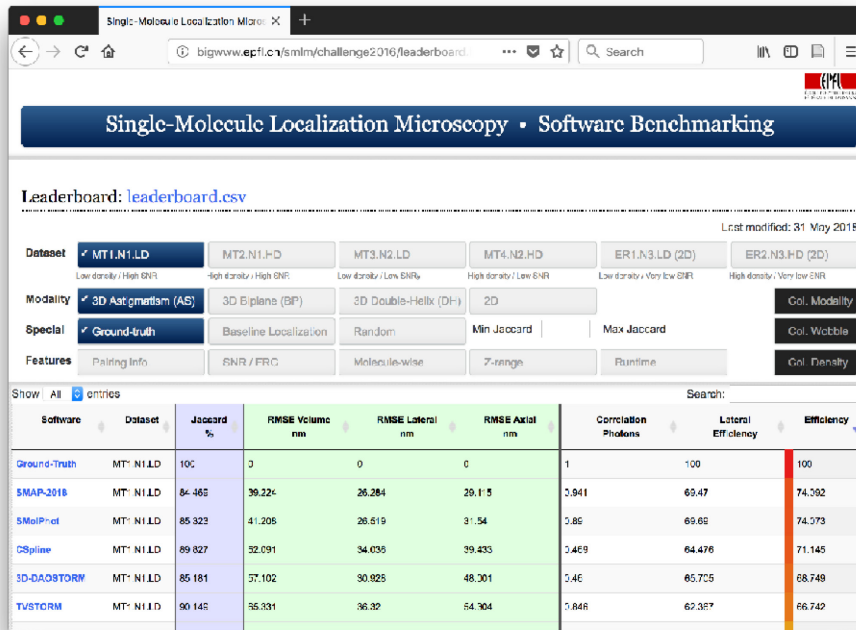
143 constructed as described in Online Methods, and under conditions summarized in Table S4. Gibson-

144 Lanni model PSF calculated under corresponding conditions (NA 1.49, 700 nm emission wavelength).

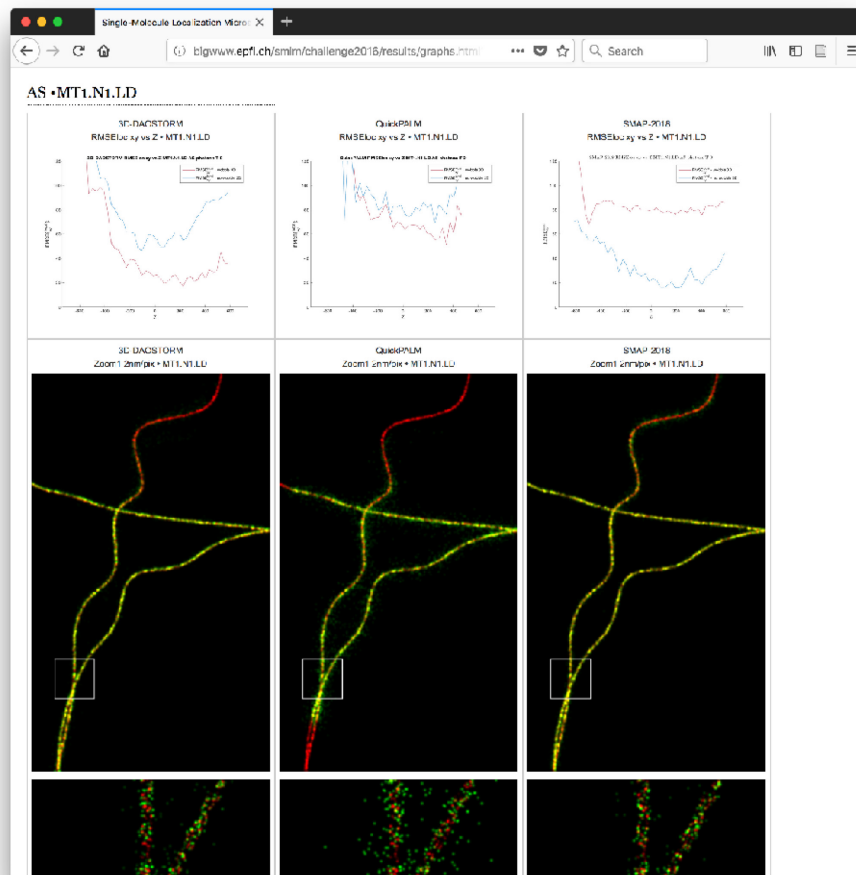
145

146

A

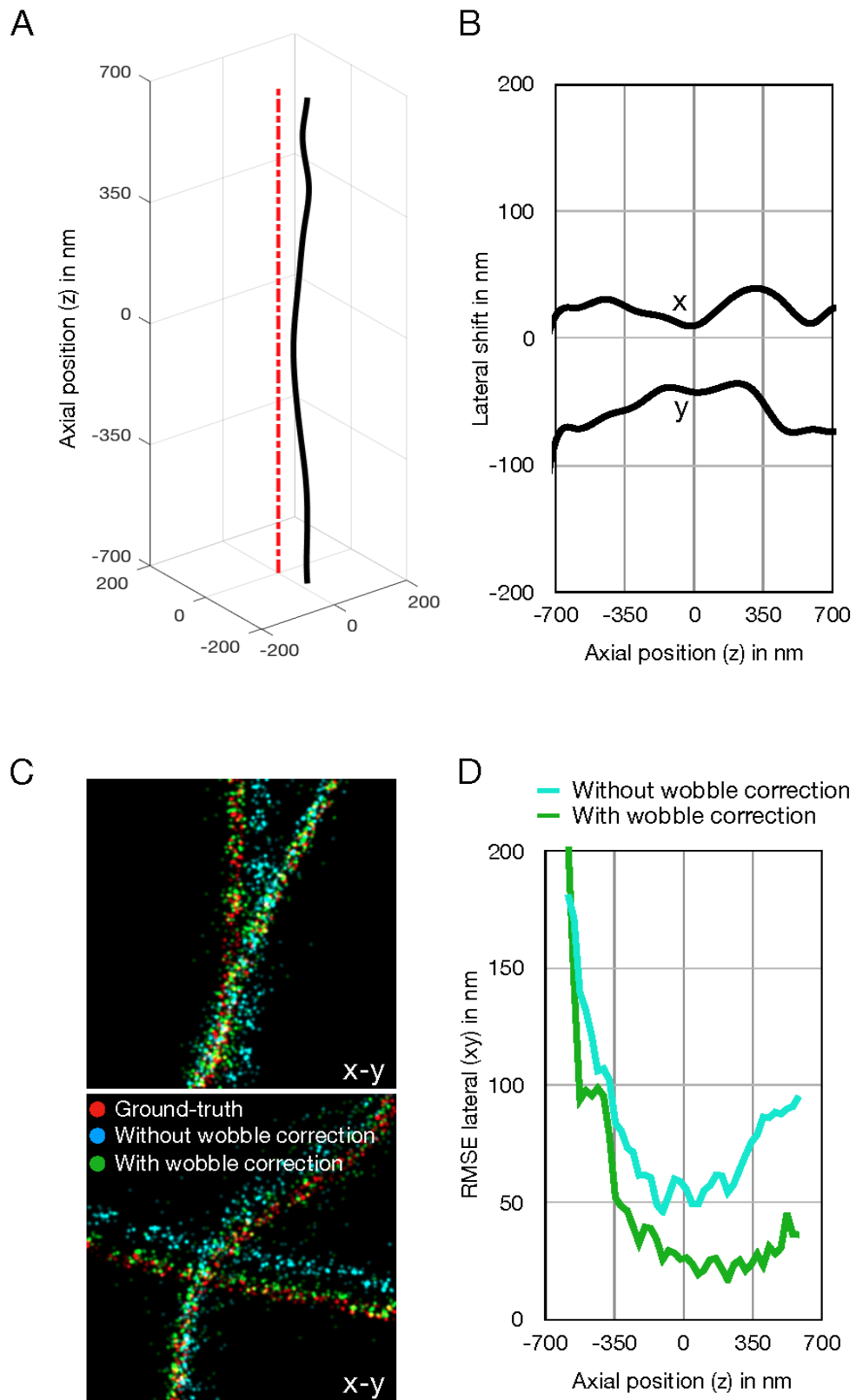


B



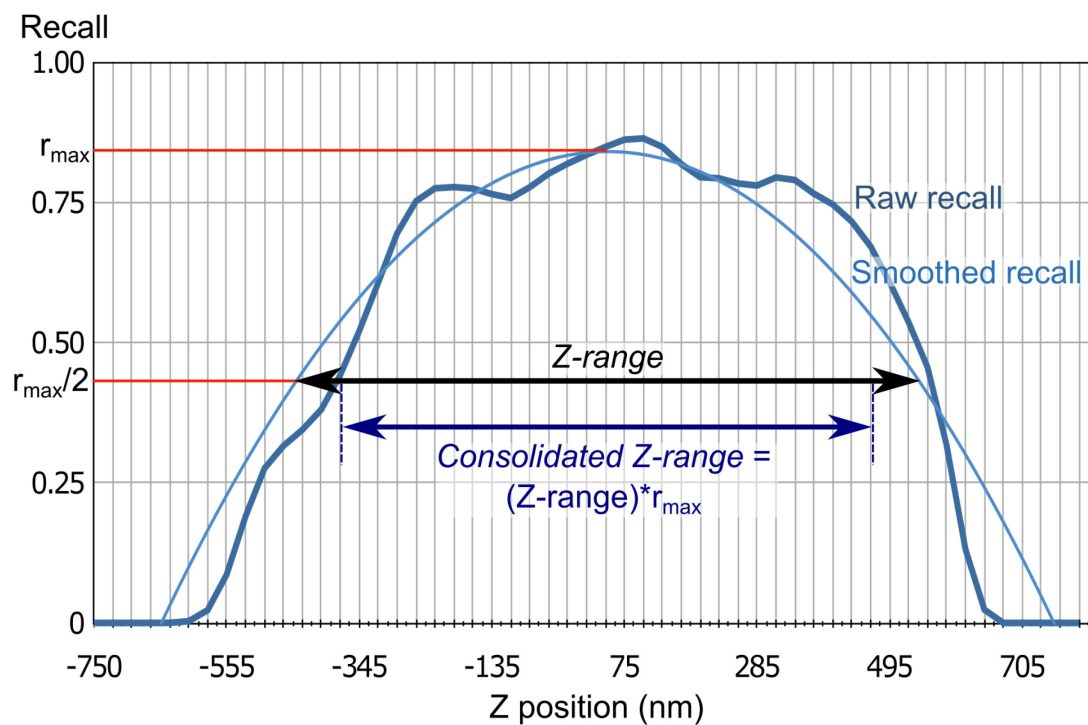
147
148
149
150
151
152

Figure S10: Screenshot of the interactive leaderboard on competition website. **A.** Software can be ranked for all key competition parameters and is automatically updated on submission of new software entries. **B.** Software can be compared side-by-side for all key competition



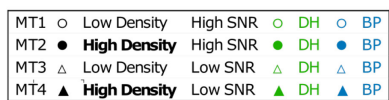
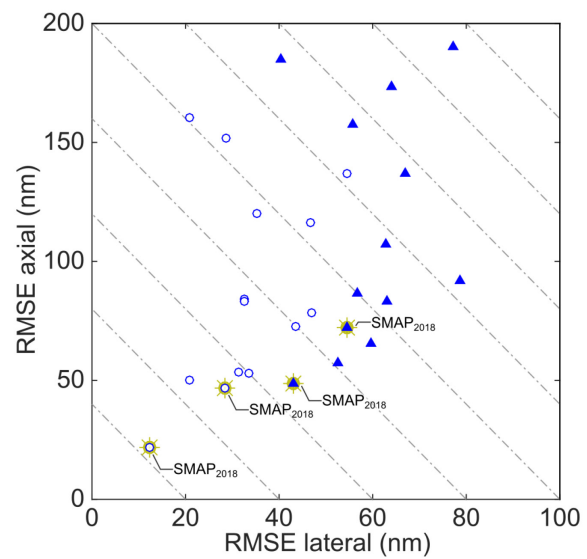
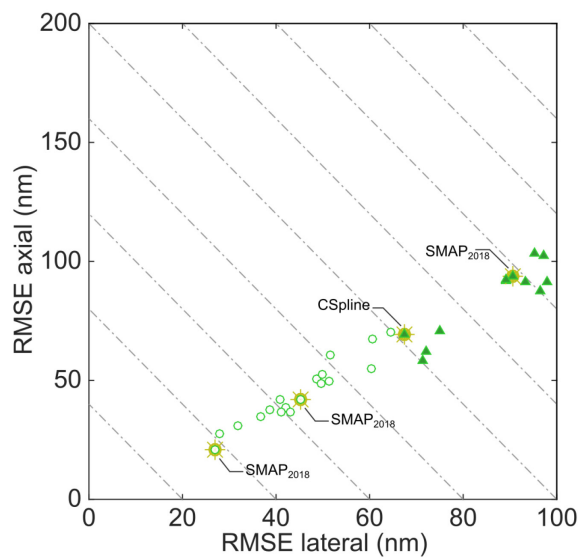
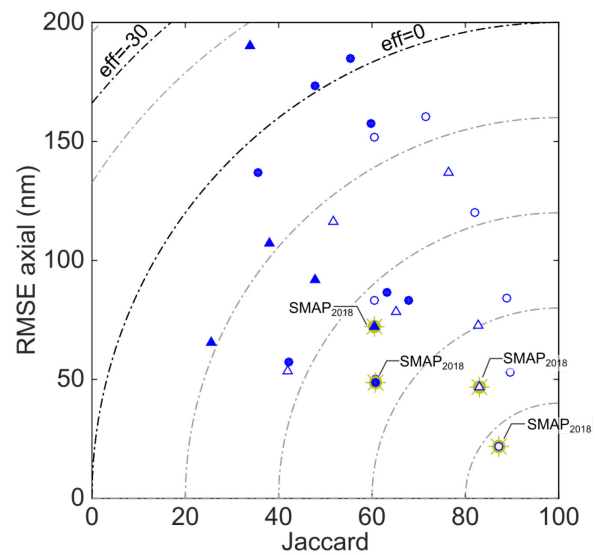
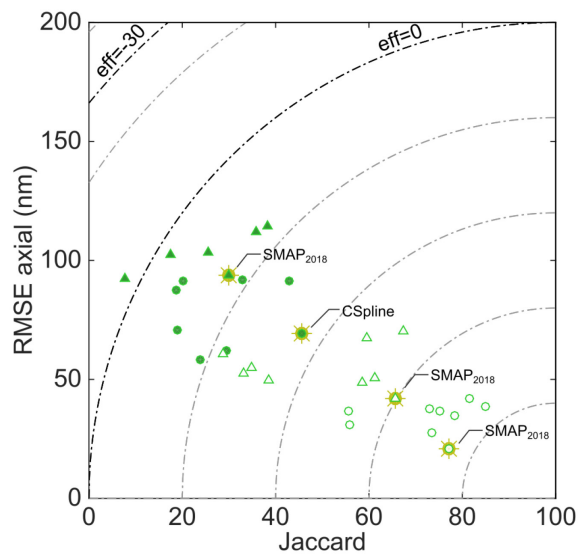
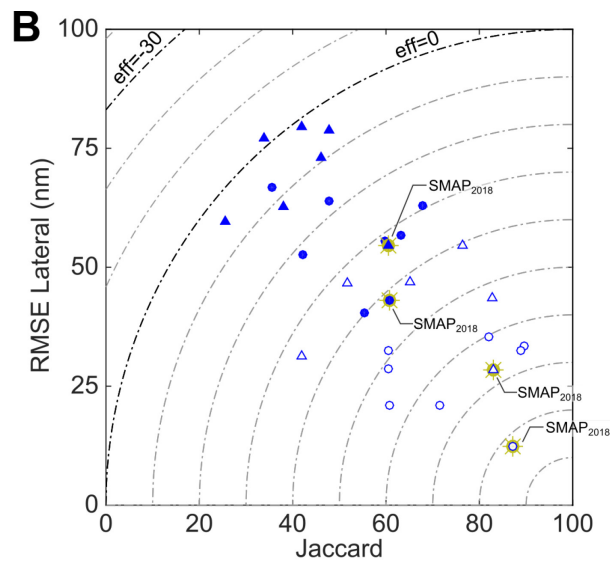
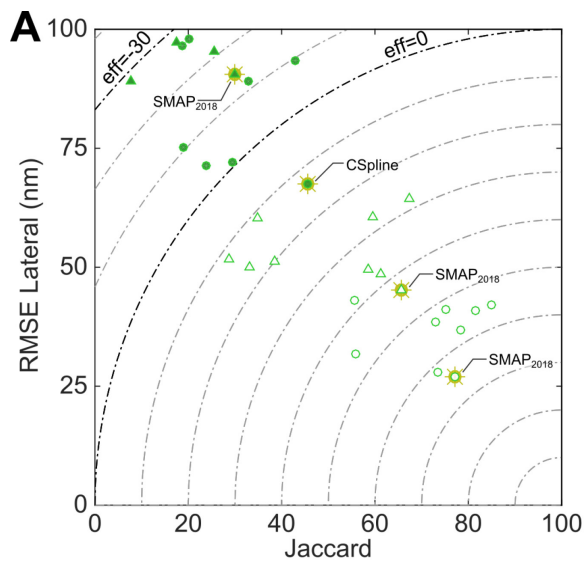
154 **Figure S11:** Wobble correction is required for accurate software-simulation comparison with
155 experimentally derived PSFs (unless the software incorporates wobble directly in the analysis
156 model). **A-B.** Profile of representative software localization offset as a function of axial position. **C-D.**
157 Comparison of representative software versus ground truth results with and without wobble
158 correction.

159



160
 161 **Figure S12:** Metrics for software Z-range. *Z-range* measures the range over which software detects
 162 $>0.5 * (\text{max recall})$ of ground truth molecules. However, a large *Z-range* is not practically useful if the
 163 software maximum recall is very low. The supplementary metric *consolidated Z-range* rescales the
 164 FWHM recall by the maximum recall. This will return a low value if either the FWHM recall or the
 165 maximum recall of the software is low.

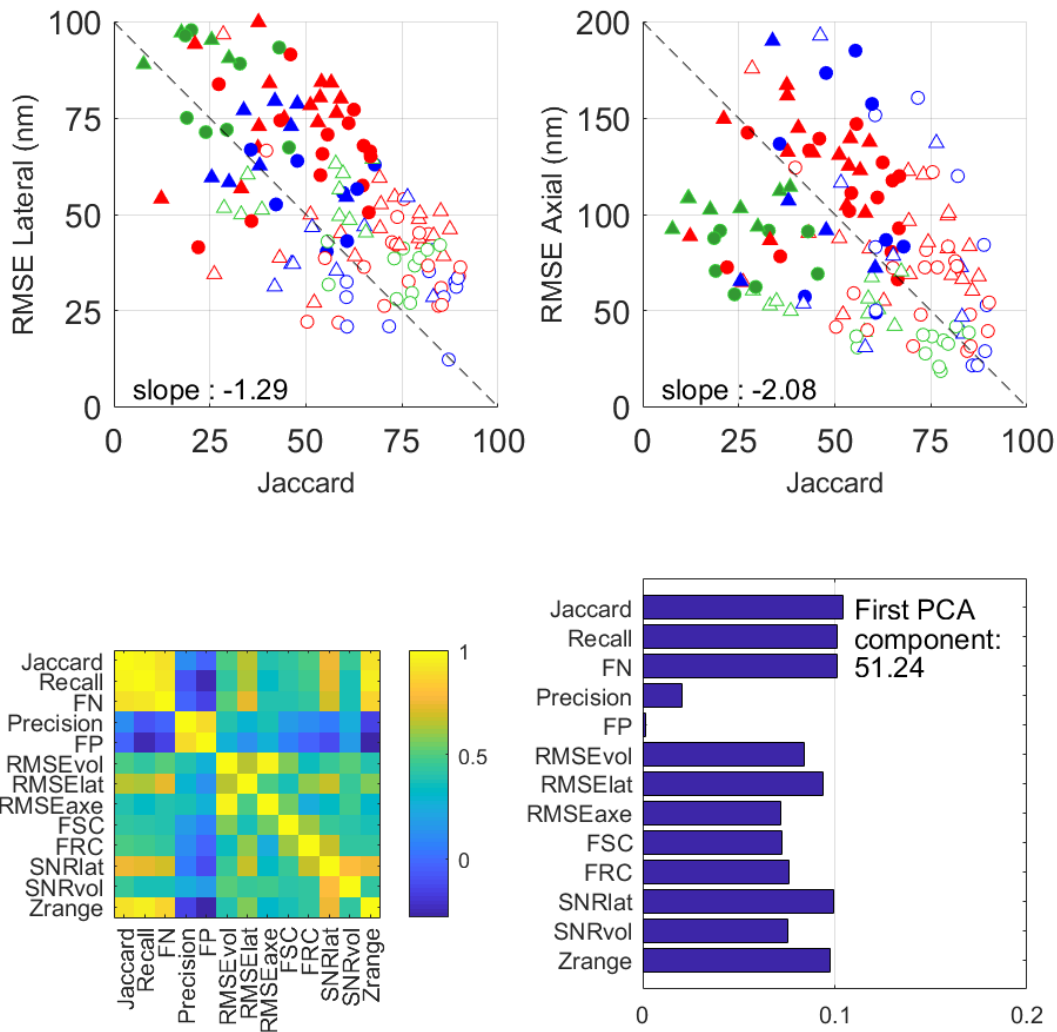
166



169

170 **Figure S13:** 3D software performance for biplane (A, BP) and double helix (B, DH) modalities. Gold
171 stars indicate top performers for each dataset. Dashed lines in top, middle panels indicate overall
172 efficiency (higher is better).

173



174

175 **Figure S14:** Comparison and principal component analysis of assessment metrics. **A.** The
 176 linear regression slope between lateral/ axial RMSE versus Jaccard index for all results
 177 (datasets and software). The weighting for the efficiency formulae relies on these
 178 observations. **B.** Covariance matrix (left) and principal component analysis (PCA, right) of
 179 the metrics for all the results. The covariance analysis shows the Jaccard index, Recall, FN,
 180 and Zrange are strongly correlated. Similarly, the different RMSEs are also correlated. To a
 181 lesser extent, the SNRs are correlated to the Jaccard index. The PCA shows that the first
 182 component explains 51.24% of the variance, which confirms there is redundancy in the
 183 metrics.

184

Name of the software	2D	2D	AS	AS	BP	BP	DH	DH	Wobble	PSF	Temporal grouping	Run-time	Grid	Specific information on the algorithm or the PSF
	LD	HD	LD	HD	LD	HD	LD	HD						
Ranked if efficiency larger than	50	30	40	10	40	10	40	10						
Non-iterative														
3D-WTM ⁶	21	11	12	9					bead	Wedge	No	<1h. GPU	#	Detection, wedge matching
QuickPALM ⁷									bead	Gauss	No	<1min.	C	Center of gravity
WTM ⁶										Wedge	No	<10min. GPU	#	Detection, wedge matching
Single emitter fitting														
3D-STORM-Tools ⁷	8		8	6					bead	Gauss	No	<10s. GPU	C	LS
EasyDHPSF ⁸							6		bead	Gauss	No	<3h	C	LS
FIRESTORM ²	22									Gauss	No	<1min.	C	LS
Localizer ⁹	17									Gauss	No	<10s. GPU	C	LS, MLE
MiaLang ¹⁰										Gauss	No	n.a.	C	MLE
MIATool ¹¹	20		13		2		5		bead	Bessel	Yes	<10min.	C	MLE
mlePALM	6		11						bead	Gauss	No	<3h.	C	MLE
Octane ¹²										Gauss	No	<1min.	C	LS
PALMER ¹³										Gauss	No	<10min. only HD	C	MLE
PeakSelector ¹⁴										Gauss	No	<10min.	C	LS
QC-STORM	14		11				7		auto	Gauss	Yes	<1s. GPU	C	MLE
RapidSTORM ¹⁵	16								bead	Gauss	No	<10s.	C	LS, MLE
SFP_Estimator	19									Gauss	No	<1min FGPA	C	MLE
SMAP-2016	10	6	7	7	3		2		bead	Gauss	Yes	<1min. GPU	C	Several algorithms, LS, MLE
SMAP-2018 ¹⁶	23		2		1	1	1		auto	Learn	Yes	<1min. GPU	C	Cubic spline representation
SMolPhot	4		1	1					auto	Gauss	Yes	<10min.	C	LS + CLEAN + Frame grouping
STORMChaser									auto	Gauss	No	<10min.	C	LS
WaveTracer ¹⁷	7		6	10					auto	Gauss	No	<1h GPU	C	LS
Multi-emitter fitting														
3D-DAOSTORM ¹⁸	2	4	4	2					bead	Gauss	Yes	<10min.	C	MLE
CSpline ¹⁹	5	9	3	3			3	1	auto	Learn	Yes	<10min.	C	Cubic spline representation
PeakFit	1	5								Gauss	No	<10min.	C	LS, MLE
RainSTORM ²⁰	12	8							bead	Gauss	No	<10min. GPU	C	LS
ThunderSTORM ²¹	9		9	5	4	4			bead	Gauss	No	<1min.	C	Several algorithms, LS, MLE
Compressed sensing 1: Matching pursuit algorithms for molecule candidates, sparsity constraint														

ADCG ²²	3	1								Gauss	No	<10min. GPU	C	Constrained gradient descent
SMfit	11	3								Gauss	No	<3h	C	Block coordinate descent
SOLAR_STORM						4			bead	Arbitrary	No	<10min.	C	Orthogonal Matching Purs. + L1H
TVSTORM ²³	15	7	5	4					bead	Gauss	No	<1h GPU	C	Backtracking line search
Compressed sensing 2: Deconvolution-type algorithm, sparsity constraint														
CELO ²⁴		12								Arbitrary	No	<3h only HD	#	Majorization- Minimization (10)
FALCON ²⁵	13	2				3			auto	Gauss	No	<3h GPU	C	Sparsity constraint (weighted 11)
L1H ²⁶										Gauss	No	<10min.	#	L1-homotopy
Other approaches														
ALOHA ²⁷										Gauss	No		C	Detection, annihilating filter
BreCs									auto	Arbitrary	No	<1h. GPU	#	Bayesian
LEAP ²⁸					3	2			auto	Bessel	No	<3h	C	Deconvolution, annihilating filter
pSMLM-3D ²⁹	18	10		8					bead	Gauss	No	<10s.	C	Detection, phasor analysis
Participation	31	28	17	14	9	8	10	9						

186 **Table S1. Participant software summary.** A grey cell in the table indicates the participation to the
187 competition and the number shows the rank of the software for on the 8 categories. The column
188 “Wobble 3D” indicates how the software proceeds with the wobble correction: **auto** for an intrinsic
189 correction, **bead** for an explication calibration on beads. The “C” in the column Grid indicates that the
190 software use a grid-less algorithm contrarily to “#” that indicates an algorithm running on a pre-
191 defined grid. The runtime is computed as much as possible by averaging the computation time
192 provided by the participants on the low density datasets (~20'000 frames) for 2D and AS, GPU indicates
193 that the participants have used a graphics processor card.

194
195

196
197

Dataset	Template structure	Sample thickness	SNR	Sample labelling method & fluorophore	Molecule brightness	Autofluorescence level	Molecule density
					photon/ mol/ frame	photons/pixel/ frame	mol/ μm
Beads	Beads calibration sample	1.5	Very high	Very bright fluorescent beads	20000	0	
MT1.N1.LD	Microtubules Diameter 25 nm	1.5	High	Organic dye (Alexa 647), antibody labelling	5000	~100 (moderate)	0.25 (low)
MT2.N1.HD		1.5	High	Organic dye (Alexa 647), antibody labelling	5000	~100 (moderate)	2.5 (high)
MT3.N2.LD		1.5	Low	Fluorescent protein label (mEos3.2)	500	~10 (low)	0.25 (low)
MT4.N2.HD		1.5	Low	Fluorescent protein label (mEos3.2)	500	~10 (low)	2.5 (high)
ER1.N3.LD	Pseudo endoplasmic reticulum. Diameter 150 nm (approximative)	0.7	Medium	Affinity dye label (Mitotracker red)	3000	~500 (high)	0.5 (low)
ER2.N3.HD		0.7	Medium	Affinity dye label (Mitotracker red)	3000	~500 (high)	5 (very high)

198 **Table S2: Simulation parameters for each condition.** Molecule density calculated based on
 199 approximate diffraction limited area (A) of structure. For a thin linear structure, $A = n \cdot L \cdot \text{FWHM}$
 200 where n is the number of filaments, L is the length of filament (approximated as image width),
 201 FWHM is PSF FWHM. For a thick linear structure, $A = n \cdot L \cdot \sqrt{w^2 + \text{FWHM}^2}$

202
203
204

Density	Structure	Role	Modality			
			2D	AS	DH	BP
	Beads	Calibration	Beads	Beads	Beads	Beads
Low Density (LD)	MT0	Training	MT0.N1.LD	MT0.N1.LD	MT0.N1.LD	MT0.N1.LD
	ER1	Contest	ER1.N3.LD			
	MT1	Contest		MT1.N1.LD	MT1.N1.LD	MT1.N1.LD
	MT3	Contest	MT3.N2.LD	MT3.N2.LD	MT3.N2.LD	MT3.N2.LD
High Density (HD)	ER2	Contest	ER2.N3.HD			
	MT2	Contest		MT2.N1.LD	MT2.N1.LD	MT2.N1.LD
	MT4	Contest	MT4.N2.HD	MT4.N2.HD	MT4.N2.HD	MT4.N2.HD

205 **Table S3: List of all competition datasets.** Datasets are available at
 206 <http://bigwww.epfl.ch/smlm/challenge2016/index.html?p=datasets>

207
208

209

Modality	Objective	Camera	Pixel size at the sample plane	Z-step	Z-range
2D	Nikon NA 1.49 TIRF oil (commercial N-STORM microscope)	EMCCD	43 nm (1.5x Optovar and 2.5x SIM magnifiers in place)	10nm	3 μ m
Astigmatism (AS)	Nikon NA 1.49 TIRF oil	EMCCD	160 nm	10nm	3 μ m
Double-helix (DH)	Nikon NA 1.49 TIRF oil	EMCCD	160 nm	20nm	3 μ m
Biplane (BP)	The biplane model PSF was constructed from the 2D PSF. The two defocused PSFs were constructed by duplicating the 2D PSF and offsetting it by -250 nm and 250 nm for each Z-plane				

210

211

212

Table S4: Microscope acquisition parameters for experimental PSF acquisition for each imaging modality.

213

214
215
216

Dataset	Modality	Participants	Winner	Jaccard Average (%)	RMSE Lateral Average (nm)	RMSE Axial Average (nm)	Jaccard Winner (%)	RMSE Lateral Winner (nm)	RMSE Axial Winner (nm)	Z-range winner (nm)	Consolidated Z-range winner (nm)
MT1.N1.LD	AS	18	SMAP-2018	73.7	38.3	66.3	84.5	26.3	29.1	1170.0	1083.897
MT2.N1.HD	AS	15	SMolPhot	52.7	66.3	109.3	66.3	50.5	66.3	849.0	665.946
MT3.N2.LD	AS	17	SMolPhot	69.3	44.9	84.0	85.8	39.2	60.3	855.0	817.127
MT4.N2.HD	AS	15	SMolPhot	43.3	77.5	128.4	58.0	76.4	100.9	851.7	623.353
MT1.N1.LD	BP	8	SMAP-2018	75.1	27.0	90.5	87.1	12.3	21.7	1198.6	1122.6
MT2.N1.HD	BP	8	SMAP-2018	54.1	55.3	116.1	60.7	43.1	48.9	1146.8	992.657
MT3.N2.LD	BP	6	SMAP-2018	66.8	41.9	84.2	83.1	28.5	46.8	1048.3	941.8
MT4.N2.HD	BP	7	SMAP-2018	41.9	69.3	134.7	60.5	54.6	72.3	1113.5	943.856
MT1.N1.LD	DH	9	SMAP-2018	72.8	36.6	34.0	77.1	27.0	20.9	1182.5	994.762
MT2.N1.HD	DH	8	CSpline	29.1	82.9	77.9	45.6	67.4	69.2	1048.1	567.954
MT3.N2.LD	DH	9	SMAP-2018	49.7	53.5	55.2	65.6	45.3	42.1	1028.3	761.962
MT4.N2.HD	DH	6	SMAP-2018	25.8	96.6	103.1	30.0	90.6	93.7	696.5	348.027
ER1.N3.LD	2D	32	ADCG	72.3	35.9	-	90.7	31.0	-	-	-
ER2.N3.HD	2D	28	ADCG	56.7	52.1	-	75.0	45.6	-	-	-
MT3.N2.LD	2D	32	SMolPhot	73.4	36.1	-	90.1	29.0	-	-	-
MT4.N2.HD	2D	29	ADCG	55.2	52.3	-	69.9	51.0	-	-	-

Table S5: Best in class and average software performance for each dataset.

217 Supplementary Note 1

218 LIST OF PARTICIPANTS TO THE CHALLENGE 2016

219

3D-DAOSTORM ¹⁸	
Contact	Hazen Babcock, Harvard University (Zhuang group), Cambridge, MA, USA
Reference	Babcock, H.P. and Zhuang, X., 2017. Analyzing single molecule localization microscopy data using cubic splines. <i>Scientific Reports</i> , 7(1), p.552.
Open-access	https://github.com/ZhuangLab/storm-analysis
Platform	Python
Class of algorithms	Multi-emitter fitting algorithm
Participation 2016	2D, AS
Note of the authors	Maximum likelihood estimation localization using a Gaussian PSF model.

3D-STORM Tools	
Contact	Fabian Hauser, CURT research group, University of Upper Austria, Linz, Austria
Open-access	Proprietary
Platform	Qt framework
Class of algorithms	Single emitter fitting
Participation 2016	2D, AS
Note of the authors	The 3D STORM Tools are easy to use applications for 3D astigmatism super-resolution microscopy. Each tool handles another domain of the 3D STORM method. The Calibration3D tool determines the calibration curves for the further steps. The Analysis3D tool evaluates 3D STORM experiments and returns a list of localizations. The Visualization3D tool offers the possibility for further 3D data analysis (e.g., clustering) and illustrates localizations of fluorophores in a 3D plot and as 2D heat-map image. All tools are written in C++ using the Qt framework version 5.7.

3D-WTM	
Contact	Shigeo Watanabe, Hamamatsu Photonics K.K., Japan
Reference	S. Watanabe et al., Evaluation of Localization Algorithm of High-Density Fluorophores, Wedged Template Matching, FOM (2013).
Open-access	Proprietary
Platform	Stand-alone (C++)
Class of algorithms	Non-iterative (Template Matching)
Participation 2016	2D, AS, DH, BP
Note of the authors	Previously we developed the Wedged Template Matching (WTM) algorithm for localizing molecules with overlapping emission point spread functions in 2D. Here we developed 3D-WTM by extending the function of WTM to 3D localization. 3D-WTM prepares template catalogue from beads z-stack images for each modality, 2D, astigmatism, double-helix and Biplane. By using the different central angle wedged shape template depending on the pixel intensity 3-WTM localizes each molecule in 3D space. After background subtraction, template matching is applied for z-axis and then sub-pixel level template matching for lateral x, y-axis localization, using normalized cross-correlation as matching evaluation function. WTM keeps applying template matching to all the information until all the molecules at images are recognized.

Contact	Nicholas Boyd, Geoff Schiebinger, Ben Recht, University of Berkeley, USA
Reference	N. Boyd, G. Schiebinger, and B. Recht. "The alternating descent conditional gradient method for sparse inverse problems." In: SIAM Journal on Optimization 27.2 (2017), pp. 616–639.
Open-access	https://github.com/nboyd/SparseInverseProblems.jl
Platform	Julia
Class of algorithms	Matching pursuit algorithm for molecule candidates, sparsity constraint
Participation 2016	2D
Note of the authors	Simple localization using the alternating descent conditional gradient method to fit Gaussians.

ALOHA	
Contact	Junhong Min and Kyong Jin, Bio-Imaging and Signal Processing Lab, KAIST, Korea
Reference	Min, J., Carlini, L., Unser, M., Manley, S. & Ye, J. C. Fast live cell imaging at nanometer scale using annihilating filter based low rank Hankel matrix approach. Wavelets and Sparsity (2015).
Platform	Matlab
Class of algorithms	Annihilating filter
Participation 2016	2D
Note of the authors	This is a grid-free 2D localization algorithm with data-driven PSF estimation. Specifically, based on the observation that the sparsity in the spatial domain implies the low-rankness in the Fourier domain, the proposed method converts PSF estimation as well as source localization problems to Fourier-domain signal processing problems so that a truly grid-free localization is possible with adaptive PSF estimation.

Brecs	
Contact	Hervé Rouault, Timothée Lionnet, Janelia Research Campus, HHMI, VA, USA
Open-access	https://github.com/hrouault/Brecs
Platform	C (Gui for ImageJ / Fiji)
Class of algorithms	Bayesian approach
Participation 2016	2D, BP, DH
Note of the authors	Several recent methods have proposed to reconstruct images at higher densities of fluorophores. However, these heuristic-based techniques are usually constrained to specific imaging schemes and are limited in their performance. We propose a rigorous formulation of the inference problem to solve, and use advanced statistical inference techniques (the Bethe approximation) to provide a controlled approximation to the exact solution. Our method, which we called B-recs (Bethe reconstruction), achieves excellent performance especially in the case of dense samples. Importantly, our technique is versatile thanks to its general and rigorous framework. We demonstrate its use with examples covering various leading edge imaging modalities, ranging from 2D superresolution to various modalities of high-density 3D imaging. A user-friendly version of our algorithm is freely available as a plugin for the popular open-source Image Analysis Software Fiji. A unique feature of B-recs is that it provides two complementary estimators for the reconstructed image: a discrete one, listing the coordinates of each fluorescent molecule detected (this is the standard output of LM algorithms); a probabilistic one, which consists of an image in which molecules appear as probability clouds which size and shape encode the localization uncertainty of each localized spot.

CELO	
Contact	Emmanuel Soubies, INRIA Sophia Antipolis, France
Reference	Soubies, E., Blanc-Féraud, L. & Aubert, G. A Continuous Exact CELO Penalty (CELO) for Least Squares Regularized Problem. <i>SIAM J. Imaging Sci.</i> 8, 1607–1639 (2015).
Platform	Matlab
Class of algorithms	Deconvolution-type algorithms with sparsity constraint
Participation 2017	2D (high-density)
Note of the authors	CELO-STORM is an algorithm designed for 2D high-density molecule localization. We formulate the localization problem as a sparse approximation problem which is then relaxed using the recently proposed CELO penalty. This relaxation is then minimized with a nonsmooth nonconvex algorithm, namely the Iterative Reweighed L1 (IRL1) algorithm.

CSpline	
Contact	Hazen Babcock, Harvard University (Zhuang group), Cambridge, MA, USA
Reference	Babcock, H. P. & Zhuang, X. Analyzing Single Molecule Localization Microscopy Data Using Cubic Splines. <i>Scientific Reports</i> 7, 552 (2017).
Open-access	https://github.com/ZhuangLab/storm-analysis/tree/master/spliner
Platform	Python
Class of algorithms	Multi-emitter fitting algorithm. Cubic-spline of the PSF.
Participation 2016	2D, AS, BP
Note of the authors	Maximum likelihood estimation using cubic-splines to model the PSF.

EasyDHPSF	
Contact	Alex von Diezmann, Camille Bayas, and W. E. Moerner, Stanford University Department of Chemistry, Stanford, USA
Reference	Lew, M. D., von Diezmann, A. R. & Moerner, W. E. Easy-DHPSF open-source software for three-dimensional localization of single molecules with precision beyond the optical diffraction limit. <i>Protocol exchange</i> 2013, (2013).
Open-access	http://sourceforge.net/projects/easy-dhpsf/files/Easy-DHPSF%20documentation%20v1.0.pdf/download
Platform	Matlab
Class of algorithms	Single emitter fitting. (only for DH)
Participation 2016	DH
Note of the authors	The fast and accurate localization of single-molecule positions from raw image data is a critical part of every single-molecule super-resolution experiment. Engineering a microscope to encode the double-helix point spread function (DH-PSF) permits excellent 3D localization precision over a ~3-micron axial (z) range, but requires specialized analysis software. Here, we present a suite of open-source MATLAB software, Easy-DHPSF, coordinated by a graphical user interface that allows the localization of single-molecule positions and reconstruction of 3D super-resolution images using the DH-PSF. For computational expediency and precision, our algorithm coarsely localizes emitters by template matching and obtains final position estimates via nonlinear least-squares fitting. A calibration of the axially-dependent revolution of the lobes of the DH-PSF is used to extract z, with xy calculated from the midpoint of the lobes plus a z-dependent correction factor. While overlapping PSFs are ignored, and the least-squares algorithm is not as precise as maximum-likelihood-estimation methods, Easy-DHPSF has been shown to obtain transverse (axial)

	localization precisions in cells of 14 (25) nm using synthetic dyes* and 28 (43) nm with fluorescent proteins, with typical processing speeds of 10s of fit PSFs per second on a standard workstation. Our software provides intuitive user-defined filters to reject false positives and refine the data, is capable of drift correction via fiducials, and can provide visual reconstructions of data as a histogram or scatterplot.
--	--

FALCON	
Contact	Junhong Min and Jong Chul Ye, Bio-Imaging and Signal Processing Lab, KAIST, Korea
Reference	Min, J. et al. FALCON: fast and unbiased reconstruction of high-density super-resolution microscopy data. Scientific reports 4, 4577 (2014).
Open-access	http://bispl.weebly.com/super-resolution-microscopy.html
Platform	Matlab
Class of algorithms	Deconvolution-type algorithms with sparsity constraint
Participation 2016	2D, DH
Note of the authors	This is a localization algorithm for high-density imaging. Our algorithm is designed to provide unbiased localization on continuous space and high recall rates for high-density imaging, and to have orders-of-magnitude shorter run times compared to previous high-density algorithms. 3D localization is also possible.

FIRESTORM	
Contact	Jochen Michael Reichel, Thomas Vomhof, Jens Michaelis, Institute of Biophysics, Ulm University, Germany
Reference	Schoen, M. et al. Super-resolution microscopy reveals presynaptic localization of the ALS/FTD related protein fus in hippocampal neurons. Frontiers in cellular neuroscience 9, 496 (2016).
Open-access	https://www.uni-ulm.de/nawi/nawi-biophys/forschung/forschung-michaelis/method-development/software/firestorm.html
Platform	Matlab
Class of algorithms	Single emitter fitting
Participation 2016	2D
Note of the authors	FIRESTORM is a localization microscopy data analysis and reconstruction tool. After background correction by a running median temporal filter regions of interest around intensity peaks are determined if the peaks meet the minimal thresholds defined by the user (max FWHM, symmetry constant, SNR, min. Number of photons). Within those regions of interest a two-dimensional Gaussian function is fitted for the intensity distribution. Blinking events spanning consecutive frames can be combined to a single blinking event with a higher number of photons. The localization list is analyzed to determine the distributions of SNR and PSF width as well as the photon statistics. Based on this analyses the localizations list can be filtered prior to the reconstruction to yield optimal trade-off between recall and localization precision. The intensity values of the reconstructed image can be chosen to be based on the number of photons (NOP) or the number of localizations (NOL). Drift can be corrected by FIRESTORM either by Redundant Cross Correlation (RCC) or by using fiducial marker positions. The program supports multi-color imaging. For sequential imaging of different colors the drift between the measurements is interpolated for the measurement pause. The software is implemented in MATLAB using parallel computation to increase analysis speed.

L1H	
Contact	Hazen Babcock, Harvard University (Zhuang group), Cambridge, MA, USA
Reference	Babcock, H. P., Moffitt, J. R., Cao, Y. & Zhuang, X. Fast compressed sensing analysis for super-resolution imaging using L1-homotopy. <i>Optics express</i> 21, 28583–28596 (2013).
Open-access	http://zhuang.harvard.edu/software/l1h.html
Platform	Python
Class of algorithms	Deconvolution-type algorithms with sparsity constraint
Participation 2016	2D
Note of the authors	Compressed sensing analysis using a L1H homotopy approach.

LEAP	
Contact	Hanjie Pan, EPFL, Lausanne, Switzerland
Reference	Pan, H., Simeoni, M., Hurley, P., Blu, T. & Vetterli, M. LEAP: Looking beyond pixels with continuous-space Estimation of Point sources. <i>A&A</i> 608, A136 (2017).
Open-access	https://github.com/hanjiepan/LEAP
Platform	Matlab
Class of algorithms	Annihilating filter
Participation 2017	BP

Localizer	
Reference	Dedecker, P., Duwé, S., Neely, R. K. & Zhang, J. Localizer: fast, accurate, open-source, and modular software package for superresolution microscopy. <i>Journal of biomedical optics</i> 17, 126008 (2012).
Open-access	http://www.igorexchange.com/project/Localizer
Platform	Igor
Class of algorithms	Single emitter fitting
Participation 2016	2D, BP (run by an expert)
Note of the authors	We present Localizer, a freely available and open source software package that implements the computational data processing inherent to several types of superresolution fluorescence imaging, such as localization (PALM/STORM/GSDIM) and fluctuation imaging (SOFI/pcSOFI). Localizer delivers high accuracy and performance and comes with a fully featured and easy-to-use graphical user interface but is also designed to be integrated in higher-level analysis environments. Due to its modular design, Localizer can be readily extended with new algorithms as they become available, while maintaining the same interface and performance. We provide front-ends for running Localizer from Igor Pro, Matlab, or as a stand-alone program. We show that Localizer performs favorably when compared with two existing superresolution packages, and to our knowledge is the only freely available implementation of SOFI/pcSOFI microscopy. By dramatically improving the analysis performance and ensuring the easy addition of current and future enhancements, Localizer strongly improves the usability of superresolution imaging in a variety of biomedical studies.

MiaLang	
Contact	Yujie Wang, Britton Chance Center for Biomedical Photonics Wuhan National Laboratory for Optoelectronics (WNLO) Huazhong University of Science and Technology, China

Reference	Quan, T. et al. Ultra-fast, high-precision image analysis for localization-based super resolution microscopy. Optics Express 18, 11867–11876 (2010).
Open-access	http://bmp.hust.edu.cn/srm/
Platform	ImageJ
Class of algorithms	Single emitter fitting
Participation 2016	2D
Note of the authors	MaLiang (Maximum likelihood algorithm and a Graphics Processing Unit) is a practical method for processing sparse isolated images of localization microscopy. It is the combination of GPU parallel computation, maximum likelihood estimator. This software is an ImageJ plugin based on parallel computation, while executes more than 8 orders of magnitudes faster.

MIATool	
Contact	R. Velmurugan, A. V. Abraham, and R. J. Ober, Texas A&M University, College Station, Texas, USA
Reference	Chao, J., Ward, E. S. & Ober, R. J. A software framework for the analysis of complex microscopy image data. IEEE Trans Inf Technol Biomed 14, 1075–1087 (2010).
Open-access	http://www.wardoberlab.com/software/miatool/
Platform	Java
Class of algorithms	Single emitter fitting
Participation 2016	2D, AS, BP, DH
Note of the authors	We present the latest implementation of the Microscopy Image Analysis Tool (MIATool) software framework and its application to single molecule localization microscopy data analysis. The MIATool framework is founded on the idea of using different logical arrangements of image pointers, as well as corresponding arrangements of processing settings, metadata, and analytical results, to facilitate the execution of the disparate tasks that are potentially required by a proper analysis of the image data. Here, we demonstrate the use of the latest realization of MIATool, coded in Java, to perform the tasks necessary for the localization-based super-resolution reconstruction of cellular structures. In particular, we illustrate how the paradigm of image pointer and associated arrangements can naturally be exploited and extended to support the analysis tasks that are carried out to properly reconstruct a high resolution image from the raw image data. These tasks include, for example, the viewing of the raw image data as a visual quality check, spot detection that identifies the single molecules, and the accurate localization of the identified molecules. A key feature of the current MIATool implementation is its flexibility. The crucial task of molecule localization, for example, can be performed with different estimation algorithms, point spread function models, and detector noise models. Analysis of data generated by different modalities, such as astigmatic imaging and multifocal plane imaging, is therefore readily supported.

mlePALM	
Contact	Hendrik Deschout, Laboratory of Nanoscale Biology, EPFL, Switzerland
Platform	Matlab
Class of algorithms	Single emitter fitting
Participation 2016	2D, AS
Note of the authors	mlePALM is an adapted version of the localization software used by Betzig et al. in their first report on Photo-Activated Localization Microscopy. We have replaced the fast but sub-optimal Gaussian mask estimator with the

	maximum likelihood estimation of a Gaussian PSF model, as implemented by Smith et al. This not only allowed us to obtain more precise localizations, but additionally enabled us to perform astigmatic 3D localization by using a bivariate Gaussian PSF model.
--	---

Octane	
Reference	Niu, L. & Yu, J. Investigating Intracellular Dynamics of FtsZ Cytoskeleton with Photoactivation Single-Molecule Tracking. <i>Biophysical Journal</i> 95, 2009–2016 (2008).
Open-access	https://github.com/jiyuuchc/Octane
Platform	ImageJ
Class of algorithms	Single emitter fitting
Participation 2016	2D (run by an expert)
Note from the website	The Octane is a program we developed to facilitate works involved in super-resolution optical imaging (PALM, STORM etc). By providing an intuitive graphical user interface front end, we hope it can serve as a useful tool for a wide range of scientists, including experimental biologists as well as physicists. The program runs as a plugin of the (extremely versatile) ImageJ software, thus can be used on any image format that is supported by ImageJ,

PALMER	
Contact	Zhen-li Huang and Yi-na Wang, Wuhan Laboratory for Optoelectronics, HUST, Wuhan, China
Reference	Wang, Y., Quan, T., Zeng, S. & Huang, Z.-L. PALMER: a method capable of parallel localization of multiple emitters for high-density localization microscopy. <i>Opt. Express</i> , OE 20, 16039–16049 (2012).
Open-access	http://bmp.hust.edu.cn/srm/
Platform	ImageJ
Class of algorithms	Single emitter fitting
Participation 2016	2D

PeakFit	
Contact	Alex Herbert and Anthony M. Carr, Genome Damage and Stability Centre, University of Sussex, UK
Open-access	http://www.sussex.ac.uk/gdsc/intranet/microscopy/imagej/smlm_plugins
Platform	ImageJ
Class of algorithms	Multi-emitter fitting
Participation 2016	2D
Note of the authors	We present software for single-molecule localisation microscopy based on 2D Gaussian fitting. For each frame candidate peaks are ranked and sequentially fit using a local region. An estimate of the PSF width is required which can be obtained from the optical system used for acquisition, or from a calibration image. Candidates are identified using smoothing on the image followed by non-maximal suppression. Peaks are processed in descending height order and fit using a region size based on the PSF width. Fitting uses Least Squares Estimation or Maximum Likelihood Estimation with an EM CCD noise model. Results are filtered using signal-to-noise, width, coordinate shift and localisation precision criteria. Processing is stopped based on consecutive failures. High density samples can add neighbour peaks within the fit region and these are included if they are within a fraction of the height of the candidate. If multiple peak fitting fails then single peak fitting is used. Additionally, the

	candidate can be fit using a two peaks model if the fit residuals show a skewed distribution in the quadrants around the centre. The doublet fit is selected if it improves the Bayesian Information Criterion (BIC). The software is written as a multi-threaded Java library and runs as a suite of plugins for ImageJ. Plugins are provided for fitting single images or an image series, drift correction and clustering, and are fully scriptable within the ImageJ macro language allowing automated analysis. Results can be visualized as a rendered image and saved to file.
--	---

PeakSelector	
Reference	Shtengel, G. et al. Interferometric fluorescent super-resolution microscopy resolves 3D cellular ultrastructure. <i>Proceedings of the National Academy of Sciences</i> 106, 3125–3130 (2009).
Platform	IDL
Class of algorithms	Single emitter fitting
Participation 2016	2D (run by an expert)
Note of the authors	PeakSelector is a software written in IDL for processing single-molecule localization microscopy. It supports grouping, visualization, filtering, 3D (astigmatism). It has a graphical user interface and runs on any platform that supports the IDL Virtual Machine.

pSMLM-3D	
Contact	Koen Martens and Johannes Hohlbein, Laboratory of Biophysics, Wageningen University, The Netherlands
Reference	Martens, K. J. A., Bader, A. N., Baas, S., Rieger, B. & Hohlbein, J. Phasor based single-molecule localization microscopy in 3D (pSMLM-3D): An algorithm for MHz localization rates using standard CPUs. <i>The Journal of Chemical Physics</i> 148, 123311 (2017).
Open-access	https://github.com/kjamartens/thunderstorm/tree/phasor-intensity-1/Compiled%20plugin
Platform	ImageJ
Class of algorithms	Detection and phasor analysis
Participation 2016	2D, AS
Note of the authors	We present a fast and model-free 2D and 3D single-molecule localization algorithm that allows more than 3×10^6 localizations per second to be calculated on a standard multi-core central processing unit with localization accuracies in line with the most accurate algorithms currently available. Our algorithm converts the region of interest around a point spread function to two phase vectors (phasors) by calculating the first Fourier coefficients in both the x- and y-direction. The angles of these phasors are used to localize the center of the single fluorescent emitter, and the ratio of the magnitudes of the two phasors is a measure for astigmatism, which can be used to obtain depth information (z-direction). Our approach can be used both as a stand-alone algorithm for maximizing localization speed and as a first estimator for more time consuming iterative algorithms.

QC-STORM	
Contact	Luchang Li, Wuhan National Laboratory for Optoelectronics-Huazhong University of Science and Technology, China
Platform	ImageJ
Class of algorithms	Single emitter fitting
Participation 2017	2D, AS, DH

Note of the authors	QC-STORM are Micro-manager and ImageJ plugins for real time processing of sCMOS based high-throughput single molecule localization imaging. QC-STORM is dramatically faster than similar software without sacrifice localization precision.
---------------------	---

QuickPALM	
Contact	Ricardo Henriques, LMCB - MRC Laboratory for Molecular Cell Biology, UCL, UK
Reference	Henriques, R. et al. QuickPALM: 3D real-time photoactivation nanoscopy image processing in ImageJ. Nat Meth 7, 339–340 (2010).
Open-access	https://code.google.com/archive/p/quickpalm/downloads
Platform	ImageJ
Class of algorithms	2D, AS
Participation 2016	Non-iterative (center of mass)
Note of the authors	QuickPALM is the first open source, freely available, ImageJ based super-resolution algorithm for 3D PALM and STORM based image analysis. Published in 2010, it rapidly became one of the most popular SMLM analytical solutions due to its speed and ease of use. It combines real-time processing capability with additional important features including 3D reconstruction, drift correction and real-time acquisition control. Contrary to most SMLM algorithms which use a fitting procedure for particle localization, QuickPALM uses an optimized and high-speed center-of-mass calculation. Since its release, QuickPALM has become one of the comparison standards for new super-resolution analysis algorithms in the field.

RainSTORM	
Contact	G. Tamas and J. Sinko, University of Cambridge UK & University of Szeged, Hungary
Reference	Rees, E. J., Erdelyi, M., Schierle, G. S. K., Knight, A. & Kaminski, C. F. Elements of image processing in localization microscopy. J. Opt. 15, 094012 (2013).
Open-access	https://laser.ceb.cam.ac.uk/research/resources/our-software
Platform	Matalb
Class of algorithms	Multi-emitter fitting
Participation 2016	2D, AS, BP
Note of the authors	rainSTORM is a software written in MATLAB for evaluating single-molecule localization based microscopy measurement (PALM, (d)STORM etc.) or simulation (TestSTORM) data. Both localization and reconstruction are crucial steps in localization based microscopy image processing developed to achieve high quality final images with super-resolution. rainSTORM provides useful and unique features to analyze and filter single localizations to minimize the effects of artifacts, validate sample structures and implement high level data evaluation. The input image stack is processed using a localization algorithm (1D Single-Gaussian, 2D Single-Gaussian or 2D Multi-Gaussian) and a background estimation method (constant or linear) selected from the options on the user interface. Users can also change the fitting algorithm parameters or apply chromatic offset calibration for the different color channels. The localizations are characterized and thresholded by pre-defined (but changeable) filters. From the accepted super-resolved data table with molecule positions, a preview image is created based on a simple 2D histogram method by default. For evaluating the entire image reconstruction process a series of plots can be generated from the accepted and even from the rejected data with the most important

	properties such as photon-count distribution, accepted/rejected localization on each frame, sigma distribution or Thompson precision. We also provide a time saving feature for batch processing a whole datafolder with a pre-defined set of parameters and marker-free drift correction.
--	--

RapidSTORM	
Reference	Wolter, S. et al. rapidSTORM: accurate, fast open-source software for localization microscopy. Nat Meth 9, 1040–1041 (2012).
Open-access	http://www.super-resolution.biozentrum.uni-wuerzburg.de/research_topics/rapidstorm/
Platform	Stand-alone application
Class of algorithms	Single emitter fitting
Participation 2016	2D, AS (run by an expert)
Note of the authors	2D and astigmatic 3D single emitter fitting, least squares & MLE fitting (least squares used here). Software is optimized for high speed of analysis.

SFP_Estimator	
Contact	Manfred Kirchgessner and Frederik Gruell, Heidelberg University, Germany
Reference	Accelerating Image Analysis for Localization Microscopy with FPGAs - IEEE Conference Publication. Available at: https://ieeexplore.ieee.org/abstract/document/6044774/ . (Accessed: 23rd April 2018)
Open-access	https://github.com/ManfredKi/SFP-Estimator
Platform	Stand-alone (QT C++)
Class of algorithms	Single emitter fitting
Participation 2016	2D
Note of the authors	The Simple Fast Parallel Estimator, SFP Estimator, implements a Maximum Likelihood Algorithm that was optimized for simple computations, in order to increase computation speed. Therefore a uniform 2D Gaussian signal shape is assumed. As shown by comparisons with much slower iterative Levenbergh Marquardth fits in Matlab simulations, the detection efficiency and estimation accuracy is at least comparable. The SFP Estimator software benefits strongly from parallel execution implementing multiple threads for different tasks during image analysis, signal detection and localization. High signal density and intersecting signals define a weakness of the algorithm, but it dismisses signals that can hardly be separated automatically, in order to avoid false outputs. Even very weak signals of SNR of down to 3 can be reliably processed, but with decreased accuracy. The SFP Estimator algorithm is integrated in a very handy Gui, that implements Qt Widgets for easy user control and to display the result images. Only the few parameters are required to generate high resolution localization images: the pixel size of the input images, and the desired size of the pixels in the localization image and depending on the average signal strength the minimum threshold to accept a signal can be adjusted. Within seconds the SFP Estimator generates and displays a localization image. Even several ten thousands of signals can be quickly processed while the bottleneck is mainly defined by the number of images to be load from hard disk.

SMAP-2016	
Contact	Jonas Ries, EMBL, Heidelberg, Germany

Reference	Li, Y. et al. Real-time 3D single-molecule localization using experimental point spread functions. Nature Methods (2018). doi: 10.1038/nmeth.4661
Platform	Matlab
Class of algorithms	Single-emitter fitting algorithm
Participation 2016	2D, AS, BP, DH
Note of the authors	<p>SMAP stands for “superresolution microscopy analysis platform” and is a MATLAB based open-source software package for single-molecule localization microscopy fitting and data analysis. Its highly modular design makes extension with own plugins easy, and most of the commonly used analysis algorithms are already implemented (currently >100 plugins). To ensure intuitive and simple use in spite of the extensive functionality, we designed an efficient and configurable user interface.</p> <p>End-users find in SMAP a powerful, yet easy to use software to perform, whereas advanced users can easily incorporate their own algorithms with minimal effort.</p> <p>Features of SMAP include:</p> <ul style="list-style-type: none"> - Various GPU and CPU based localization algorithms. - Fitting during the acquisition and rendering during fitting. - 3D via astigmatism, biplane and double helix PSF. - Compatible with a variety of image formats including metadata using the OME framework. - Dual-color via sequential or ratiometric imaging. - Powerful drift correction, fast grouping. - Various modules to evaluate localization statistics and resolution including FRC. - A real-time renderer for a google-maps like browsing of data. - Rendering in several layers to overlay different channels, files, reconstruction modes or Tiff images. - A real-time 3D renderer including stereoscopic images. - A powerful ROI manager to segment and annotate ROIs and process those with various evaluation plugins. <p><i>Note:</i> This is the 2016 version entered in the first iteration of the 2016 3D SMLM challenge.</p>

SMAP-2018	
Contact	Yiming Li, Jonas Ries, EMBL, Heidelberg, Germany
Reference	Li, Y. et al. Real-time 3D single-molecule localization using experimental point spread functions. Nature Methods (2018). doi: 10.1038/nmeth.4661
Platform	Matlab
Class of algorithms	Single-emitter fitting algorithm
Participation 2016	2D, AS, BP, DH
Note	This is the 2018 version of the SMAP software corresponding to the published software. Includes fitting to experimentally derived model PSF.

SMFit	
Contact	Hayato Ikoma, Electrical Engineering Department, Stanford University, USA
Platform	Julia
Class of algorithms	Matching pursuit algorithm for molecule candidates, sparsity constraint
Participation 2016	2D
Note of the authors	Localization-based super-resolution microscopy is becoming a popular tool in biological research to clearly visualize structures at tens-of-nanometers scale. Recently, this method has been extended to handle high molecular

	<p>density images by using sparsity-inducing optimization methods. However, localization from high-density images is still a challenging task, and their performance is still limited compared to the localization from long-sequence images. Recently, another optimization algorithm, alternating descent conditional gradient method (ADCG), has been proposed to solve sparse spike deconvolution problem. In the present work, we demonstrate its practical usage for single-molecule localization microscopy on the training datasets of the localization Challenge 2016. ADCG fits multiple point spread functions to an image in a one-by-one manner, which requires analytical expression of the point spread function. This procedure suppresses false positive detections and can be performed on both 2D and 3D localization. Before applying ADCG, the input images are preprocessed with noise stabilization and background subtraction. To perform 2D localization, integrated Gaussian function is used as a point spread function.</p>
--	---

SMolPhot	
Contact	Martti Pärs, Ardi Loot, Andreas Valdmann, Marko Eltermann, Mihkel Kree, University of Tartu, Institute of Physics, Tartu, Estonia
Open-access	https://bitbucket.org/ardiloot/smolphot-software/wiki/Home
Platform	Python
Class of algorithms	Single emitter fitting
Participation 2016	2D, AS
Note of the authors	Our user friendly single-molecule localization microscopy software package features: a) preprocessors for noise filtering and background subtraction; b) uses astigmatism approach as a z-calibration tool for 3D localization; c) includes local-maxima, blob-detection and connected-component localization algorithms; d) 2D and 3D Gaussian point spread functions for fitting; e) uses post-processing which to filter molecules according to localization goodness classified by standard deviation of fitting parameters or any linear combinations of them defined by user; f) applies temporal correlation for enhancing localization accuracy by combining locations of single molecule over multiple frames. More details about our software project will be presented on (www.molphot.com).

SOLAR_STORM	
Contact	Yoon J. Jung and Nikta Fakhri, Fakri Lab, MIT, USA
Platform	Matlab / C
Class of algorithms	Matching pursuit algorithm for molecule candidates, sparsity constraint
Participation 2016	DH
Note of the authors	In super-resolution imaging techniques based on single-molecule stochastic switching, a random subset of fluorescent emitters are imaged and localized for every imaging frame. In the post-processing step, the point spread function (PSF) is used to reconstruct images by localizing molecules with high precision. Attempts to reduce the image acquisition time are based on increasing the density of emitters which fluoresce in each frame. However, as the density of excited emitters increase, PSFs start to overlap and the conventional single molecule localization techniques fail. This is particularly a bigger problem for 3D localization due to the size of the 3D PSF. Here we introduce a fast and accurate compressive sensing algorithm for localizing fluorescent emitters in high density in 3D, namely sparse support recovery using Orthogonal Matching Pursuit and L1-Homotopy algorithm for reconstructing STORM images (SOLAR STORM). SOLAR STORM reduces

	computational complexity by combining Orthogonal Matching Pursuit with L1-Homotopy, and can be accelerated by parallel implementation with GPUs. This method will allow studying dynamics of densely labeled samples in daily experiments by providing fast and robust image reconstruction.
--	--

STORMChaser	
Contact	Anna Archetti, Institute of Physics, EPFL, Switzerland
Platform	Matlab
Class of algorithms	Single emitter fitting
Participation 2016	DH
Note of the authors	Several methods have been developed for far-field single molecule (SM) localization microscopy: astigmatic imaging, double-helix (DH) point spread function (PSF), and interferometric PALM (iPALM). The DH-PSF based approach extends the axial range to approximately 2 μ m while maintaining good axial (up to 20nm) and lateral localization precisions (10nm). In order to localize the SM from the DH-PSF images many algorithms have already been implemented based on simple geometrical PSF models (least square (LS) based fitting [1] and center of mass based centroid) or those utilizing a maximum likelihood estimator (MLE). Both have their advantages (precision or speed) and have been successfully combined for traditional localization microscopy [2]. However, there exists no open-source DH-PSF localization routine that leverages the advantages of both classes of algorithm. To address this need, we are developing a fast and precise DH-PSF localization algorithm that we called STORMChaser. STORMChaser, written in a combined C++/Matlab environment, is showing promising preliminary results.

ThunderSTORM	
Contact	Martin Ovesny, Guy Hagen and Pavel Krizek, Charles University, Prague, Czech Republic
Reference	Ovesný, M., Křížek, P., Borkovec, J., Švindrych, Z. & Hagen, G. M. ThunderSTORM: a comprehensive ImageJ plug-in for PALM and STORM data analysis and super-resolution imaging. <i>Bioinformatics</i> 30, 2389–2390 (2014).
Open-access	http://zitmen.github.io/thunderstorm/
Platform	ImageJ
Class of algorithms	Multi-emitter fitting
Participation 2016	2D, AS,BP
Note of the authors	ThunderSTORM is an open-source, interactive, and modular plug-in for ImageJ designed for automated processing, analysis, and visualization of data acquired by single molecule localization microscopy methods such as PALM and STORM. ThunderSTORM offers an extensive collection of processing and post-processing methods so that users can easily adapt the process of analysis to their data. ThunderSTORM also offers a set of tools for creation of simulated data and for quantitative performance evaluation of localization algorithms using Monte-Carlo simulations.

TVSTORM	
Contact	Jiaqing Huang, The Ohio State University, Columbus, OH, USA
Reference	Huang, J., Sun, M. & Chi, Y. Super-resolution image reconstruction for high-density 3D single-molecule microscopy. in 2016 IEEE 13th International Symposium on Biomedical Imaging (ISBI) 241–244 (2016).
Platform	Matlab

Class of algorithms	Matching pursuit algorithm for molecule candidates, sparsity constraint
Participation 2016	2D, AS
Note of the authors	Single-molecule localization based super-resolution microscopy achieves sub-diffraction-limit spatial resolution by localizing a sparse subset of stochastically activated emitters in each frame. Its temporal resolution, however, is constrained by the maximal density of activated emitters that can be successfully reconstructed. The state-of-the-art three-dimensional (3D) reconstruction algorithm based on compressed sensing suffers from high computational complexity and gridding error due to model mismatch. In this paper, we propose a novel super-resolution algorithm for 3D image reconstruction, dubbed TVSTORM, which promotes the sparsity of activated emitters without discretizing their locations. Several strategies are pursued to improve the reconstruction quality under the Poisson noise model, and reduce the computational time by an order-of-magnitude. Numerical results on both simulated and cell imaging data are provided to validate the favorable performance of the proposed algorithm and its application to 2D image reconstruction.

WaveTracer	
Contact	Adel Kechkar and Jean-Baptiste Sibarita, University of Bordeaux and Institute for Neuroscience, France
Reference	Kechkar, A., Nair, D., Heilemann, M., Choquet, D. & Sibarita, J.-B. Real-Time Analysis and Visualization for Single-Molecule Based Super-Resolution Microscopy. PLOS ONE 8, (2013).
Platform	Metamorph
Class of algorithms	Single emitter fitting
Participation 2016	2D, AS
Note of the authors	WaveTracer is a module integrated into Metamorph software (https://www.moleculardevices.com/systems/metamorph-research-imaging/metamorph-microscopy-automation-and-image-analysis-software). It is an optimized framework for 2D real-time, <i>i.e.</i> , streaming, localization and reconstruction, followed, if needed, by a post-acquisition 3D reconstruction. First, the images are analysed in real-time using a wavelet based algorithm which we optimized for speed using a mix of CPU/GPU implementation. If 3D computation is required, positions and intensities of all localized molecules are stored into memory. Second, astigmatism based 3D localization is performed sequentially to the real-time reconstruction by anisotropic Gaussian fitting around the stored molecules' positions. Gaussian fittings are performed in parallel using GPU.

WTM	
Contact	Shigeo Watanabe, Jiro Yamashita, Teruo Takahashi, Tomochika Takeshima, Hamamatsu Photonics K.K. Japan
Platform	Stand-alone
Class of algorithms	Non-iterative (Template Matching)
Participation 2016	2D
Note of the authors	Multi-emitter fitting algorithms will open the door to more applications of localization microscopy including live cell super resolution microscopy by addressing a significant limitation of single molecule localization microscopy, specifically the requirement for many (typically >5,000) raw image frames to produce meaningful reconstructions. In addition to reducing the number of frames of data required, multi-fitter localization also reduces phototoxicity.

	<p>Several algorithms have been developed for multi-emitter fitting. Although these algorithms are powerful tools for reducing the number of images needed for super resolution imaging, each of these methods has its own difficulties including a low limit for the number of overlapping emission point spread functions or requiring an accurate noise model of system and detector (especially for maximum likelihood based algorithms). The computational execution time is too slow for widespread use.</p> <p>To address these issues, we developed the Wedged Template Matching (WTM) algorithm for localizing molecules with overlapping emission point spread functions. Importantly, the computation time to reconstruct a high-density final super resolution image is 20X - 1000X faster than other multi-emitter fitting algorithms, suggesting that live cell super resolution imaging will be practical. The WTM algorithm also can be applied to a 2048 x 2048 pixel sCMOS camera image.</p>
--	--

220
221
222

223 **SUPPLEMENTARY REFERENCES**

- 224 1. Ober, R. J., Ram, S. & Ward, E. S. Localization Accuracy in Single-Molecule Microscopy.
225 *Biophys. J.* **86**, 1185–1200 (2004).
- 226 2. Aguet, F., Van De Ville, D. & Unser, M. A maximum-likelihood formalism for sub-
227 resolution axial localization of fluorescent nanoparticles. *Opt. Express* **13**, 10503–10522
228 (2005).
- 229 3. Chao, J., Ward, E. S. & Ober, R. J. Localization accuracy in single molecule microscopy
230 using electron-multiplying charge-coupled device cameras. *Proc. SPIE* **8227**, (2012).
- 231 4. Chao, J., Ward, E. S. & Ober, R. J. Fisher information theory for parameter estimation in
232 single molecule microscopy: tutorial. *JOSA A* **33**, B36–B57 (2016).
- 233 5. Gibson, S. F. & Lanni, F. Experimental test of an analytical model of aberration in an oil-
234 immersion objective lens used in three-dimensional light microscopy. *JOSA A* **9**, 154–166
235 (1992).
- 236 6. Takeshima, T., Takahashi, T., Yamashita, J., Okada, Y. & Watanabe, S. A multi-emitter
237 fitting algorithm for potential live cell super-resolution imaging over a wide range of
238 molecular densities. *J. Microsc.* **0**,
- 239 7. Henriques, R. *et al.* QuickPALM: 3D real-time photoactivation nanoscopy image
240 processing in ImageJ. *Nat Meth* **7**, 339–340 (2010).
- 241 8. Lew, M. D., von Diezmann, A. R. & Moerner, W. E. Easy-DHPSF open-source software
242 for three-dimensional localization of single molecules with precision beyond the optical
243 diffraction limit. *Protoc. Exch.* **2013**, (2013).
- 244 9. Dedecker, P., Duwé, S., Neely, R. K. & Zhang, J. Localizer: fast, accurate, open-source,
245 and modular software package for superresolution microscopy. *J. Biomed. Opt.* **17**,
246 126008 (2012).
- 247 10. Quan, T. *et al.* Ultra-fast, high-precision image analysis for localization-based super
248 resolution microscopy. *Opt. Express* **18**, 11867–11876 (2010).

- 249 11. Tahmasbi, A., Ward, E. S. & Ober, R. J. Determination of localization accuracy based
250 on experimentally acquired image sets: applications to single molecule microscopy. *Opt.*
251 *Express* **23**, 7630–7652 (2015).
- 252 12. Niu, L. & Yu, J. Investigating Intracellular Dynamics of FtsZ Cytoskeleton with
253 Photoactivation Single-Molecule Tracking. *Biophys. J.* **95**, 2009–2016 (2008).
- 254 13. Wang, Y., Quan, T., Zeng, S. & Huang, Z.-L. PALMER: a method capable of parallel
255 localization of multiple emitters for high-density localization microscopy. *Opt. Express* **20**,
256 16039–16049 (2012).
- 257 14. Shtengel, G. *et al.* Interferometric fluorescent super-resolution microscopy resolves
258 3D cellular ultrastructure. *Proc. Natl. Acad. Sci.* **106**, 3125–3130 (2009).
- 259 15. Wolter, S. *et al.* rapidSTORM: accurate, fast open-source software for localization
260 microscopy. *Nat. Methods* **9**, 1040–1041 (2012).
- 261 16. Li, Y. *et al.* Real-time 3D single-molecule localization using experimental point spread
262 functions. *Nat. Methods* (2018). doi:10.1038/nmeth.4661
- 263 17. Kechkar, A., Nair, D., Heilemann, M., Choquet, D. & Sibarita, J.-B. Real-Time
264 Analysis and Visualization for Single-Molecule Based Super-Resolution Microscopy.
265 *PLOS ONE* **8**, e62918 (2013).
- 266 18. Babcock, H., Sigal, Y. M. & Zhuang, X. A high-density 3D localization algorithm for
267 stochastic optical reconstruction microscopy. *Opt. Nanoscopy* **1**, 1–10 (2012).
- 268 19. Babcock, H. P. & Zhuang, X. Analyzing Single Molecule Localization Microscopy
269 Data Using Cubic Splines. *Sci. Rep.* **7**, 552 (2017).
- 270 20. Rees, E. J., Erdelyi, M., Schierle, G. S. K., Knight, A. & Kaminski, C. F. Elements of
271 image processing in localization microscopy. *J. Opt.* **15**, 094012 (2013).
- 272 21. Ovesný, M., Křížek, P., Borkovec, J., Švindrych, Z. & Hagen, G. M. ThunderSTORM:
273 a comprehensive ImageJ plug-in for PALM and STORM data analysis and super-
274 resolution imaging. *Bioinformatics* **30**, 2389–2390 (2014).
- 275 22. Boyd, N., Schiebinger, G. & Recht, B. The Alternating Descent Conditional Gradient
276 Method for Sparse Inverse Problems. *SIAM J. Optim.* **27**, 616–639 (2017).

- 277 23. Huang, J., Sun, M., Ma, J. & Chi, Y. Super-Resolution Image Reconstruction for
278 High-Density Three-Dimensional Single-Molecule Microscopy. *IEEE Trans. Comput.*
279 *Imaging* **3**, 763–773 (2017).
- 280 24. Soubies, E., Blanc-Féraud, L. & Aubert, G. A Continuous Exact ℓ_0 Penalty
281 (CEL0) for Least Squares Regularized Problem. *SIAM J. Imaging Sci.* **8**, 1607–1639
282 (2015).
- 283 25. Min, J. *et al.* FALCON: fast and unbiased reconstruction of high-density super-
284 resolution microscopy data. *Sci. Rep.* **4**, 4577 (2014).
- 285 26. Babcock, H. P., Moffitt, J. R., Cao, Y. & Zhuang, X. Fast compressed sensing
286 analysis for super-resolution imaging using L1-homotopy. *Opt. Express* **21**, 28583–28596
287 (2013).
- 288 27. Min, J., Carlini, L., Unser, M., Manley, S. & Ye, J. C. Fast live cell imaging at
289 nanometer scale using annihilating filter-based low-rank Hankel matrix approach. in (eds.
290 Papadakis, M., Goyal, V. K. & Van De Ville, D.) 95970V (2015). doi:10.1117/12.2187393
- 291 28. Pan, H., Simeoni, M., Hurley, P., Blu, T. & Vetterli, M. LEAP: Looking beyond pixels
292 with continuous-space Estimation of Point sources. *Astron. Astrophys.* **608**, A136 (2017).
- 293 29. Martens, K. J. A., Bader, A. N., Baas, S., Rieger, B. & Hohlbein, J. Phasor based
294 single-molecule localization microscopy in 3D (pSMLM-3D): An algorithm for MHz
295 localization rates using standard CPUs. *J. Chem. Phys.* **148**, 123311 (2017).
- 296